ÉCOLE POLYTECHNIQUE FÉDÉRALE DE LAUSANNE

MATHICSE

Institute of Mathematics

School of Basic Sciences

MATHICSE Technical Report
Nr. 21.2017
September 2017

An algebraic least squares reduced basis method for the solution of parametrized Stokes equations

Niccolo Dal Santo, Simone Deparis, Andrea Manzoni, Alfio Quarteroni

http://mathicse.epfl.ch

Address: EPFL - SB – INSTITUTE of MATHEMATICS – Mathicse
(Bâtiment MA) Station 8 - CH-1015 - Lausanne - Switzerland

An algebraic least squares reduced basis method for the solution of parametrized Stokes equations

N. DAL SANTO[1], S. DEPARIS[1], A. MANZONI[1], A. QUARTERONI[1,2]

September 29, 2017

[1] CMCS, École Polytechnique Fédérale de Lausanne (EPFL),
Station 8, 1015 Lausanne, Switzerland.
[2]Mox-Laboratory for Modeling and Scientific Computing, Department of Mathematics, Politecnico di Milano, P.za Leonardo da Vinci 32, 20133 Milano, Italy (on leave).

Abstract

In this paper we propose a new, purely algebraic, Petrov-Galerkin reduced basis (RB) method to solve the parametrized Stokes equations, where parameters serve to identify the (variable) domain geometry. Our method is obtained as an algebraic least squares reduced basis (aLS-RB) method, and improves the existing RB methods for Stokes equations in several directions. First of all, it does not require to enrich the velocity space, as often done when dealing with a velocity-pressure formulation. This because it relies on a Petrov-Galerkin RB method rather than on a Galerkin RB (G-RB) method, and exploits a suitable approximation of the matrix-norm in the definition of the (global) supremizing operator. The knowledge of an analytical map between a reference domain and the physical, parameter-dependent domain, is not requested. For this reason, possible deformations of the domain which result from the solution of a computational problem can be accounted for. The new method also provides a fully automated procedure to assemble and solve the RB problem, able to treat any kind of parametrization. We prove the stability of the resulting aLS-RB problem (in the sense of a suitable inf-sup condition) and provide a numerical comparison between the proposed method and the current state-of-art G-RB methods relying on the enrichment of the velocity space. In particular, our approach results in a cheaper, more convenient option both during the offline and the online stage of computation, compared to the existing G-RB methods; numerical results are provided on a problem featuring a parameter-dependent geometry and more than 10^6 degrees of freedom regarding its high-fidelity finite element approximation.

1 Introduction

Solving saddle-point problems depending on a set of input parameters is a relevant task in several engineering contexts. In this work, as a special instance of such a problem, we consider the parametrized Stokes equations, which describe a viscous incompressible fluid when the nonlinear convective terms are neglected. The numerical solution of the Stokes equations is in general a challenging task, however a remarkable family of efficient methods exists, see e.g. [21, 32, 36]. An even more challenging task occurs when devising an efficient solver when a parametrized version of the Stokes equations is considered. This is precisely the scope of this investigation.

In this paper we deal with the efficient solution by means of the reduced basis (RB) method of parametrized steady Stokes equations of the form

$$\begin{cases} -\nu^{\boldsymbol{\mu}} \Delta \vec{u}^{\boldsymbol{\mu}} + \nabla p^{\boldsymbol{\mu}} = \vec{f}^{\boldsymbol{\mu}} & \text{in } \Omega^{\boldsymbol{\mu}} \\ \nabla \cdot \vec{u}^{\boldsymbol{\mu}} = 0 & \text{in } \Omega^{\boldsymbol{\mu}} \\ + \, b.c. \end{cases} \tag{1}$$

which can be seen as a prototypical example of parametrized saddle-point problem, modeling the velocity $\vec{u}^{\boldsymbol{\mu}}$ and the pressure $p^{\boldsymbol{\mu}}$ of a viscous incompressible fluid with viscosity $\nu^{\boldsymbol{\mu}}$ in a domain $\Omega^{\boldsymbol{\mu}} \subset \mathbb{R}^d$, $d = 2, 3$. In (1), the vector of parameters $\boldsymbol{\mu}$ describes physical and/or geometrical properties of the system, whereas $\vec{f}^{\boldsymbol{\mu}}$ is the known right hand side collecting all the data of the problem; system (1) must be supplied with proper boundary conditions, which may also depend on $\boldsymbol{\mu}$.

In particular, we are interested in the efficient solution of (1) for several (say, thousands) instances of $\boldsymbol{\mu}$. This requirement – arising, e.g., when dealing with uncertainty quantification, sensitivity analysis or PDE-constrained optimization – makes usual high-fidelity approximation techniques, such as the finite element

(FE) method, extremely expensive, if not computationally unaffordable. In fact, the FE approximation of problem (1) entails the solution of a parametrized, saddle-point (linear) system whose dimension N_h is usually very large, where h is related to the mesh size; in three-dimensional applications of real-life interest, N_h is typically of order of millions. Assembling from scratch, and then solving, the corresponding linear system for any new value of $\boldsymbol{\mu}$ is thus unfeasible. Such a task can be more easily tackled by means of reduced-order modeling techniques. Among all the available methodologies, we focus on the reduced basis (RB) method to deal with (1).

The main idea of the RB method for parameter dependent partial differential equations (PDEs) is to approximate its solution by a linear combination of few global basis functions, obtained from a set of FE solutions (or *snapshots*) corresponding to different parameter values [33, 24]. This strategy is pursued in two stages: an *offline phase* and an *online phase*. In the former, we construct a RB space V_N of dimension $N \ll N_h$ whose basis is obtained by (properly orthonormalized) linear combinations of FE solutions of the parametrized PDE. In the latter, we require the projection of the residual of the FE problem onto the RB test space to vanish, obtaining a small problem which replaces the original high-fidelity FE problem.

Initially applied to linear elliptic PDEs, the RB method has been extended to saddle-point problems such as the Stokes equations, and extensively investigated in the past decade. In particular, several works have been devoted to the analysis and the implementation of the RB method for addressing problems involving Stokes-like systems; a non-exhaustive list includes, among others: Stokes flows featuring affine [39, 23, 38] and nonaffine parameter dependence [37]; Navier-Stokes flows depending on physical and/or geometrical parameters [17, 34, 18, 26]; parametrized optimal control problems [31] or shape optimization problems [28] involving Stokes flows. In all these cases, the RB method relies on:

1. a (weak) greedy algorithm for the incremental construction of the RB space, performed by selecting a new basis for the velocity and the pressure upon the use of a residual-based a posteriori error estimator. This latter is a $\boldsymbol{\mu}$-dependent quantity related with the FE approximation and is not always easily available or computable;

2. a Galerkin projection onto the RB space to generate the RB problem (G-RB method).

Of course, this is not the only available choice. Regarding point 1., proper orthogonal decomposition (POD), rather than greedy algorithms, can be used to build the RB space. When such a strategy is employed, a set of FE solutions, called snapshots, are computed and the RB spaces for the velocity and the pressure are constructed, either jointly or separately, by performing POD, [3, 8, 12, 20, 25, 41]. This option has been considered, e.g., in [4] where two-dimensional Navier-Stokes flows on simple geometries affinely parametrized have been treated. Moreover, we remark that other possibilities have been investigated, e.g. in [19], where proper generalized decomposition (PGD) is applied to the Stokes equations in two-dimensional parametrized geometries.

Concerning point 2., a more general Petrov-Galerkin (rather than Galerkin) projection – such as in the case of a least-squares (LS) method – can be performed, choosing a test space different from the trial space, see e.g. [14, 16]. This option has been first explored in the case of two-dimensional, affinely parametrized Stokes problems on simple geometries in [1]. Moreover, in both these cases parameter-dependent domains $\Omega^{\boldsymbol{\mu}}$ were obtained as images of a reference domain Ω^0 through a parameter-dependent map whose expression was known analytically. This is a relevant limitation toward the application of RB methods to more general domains with varying shape, not necessarily obtained in an explicit way from *a priori* known, parametrized deformations[1].

What makes the RB approximation of parametrized Stokes equations hard (and, more generally speaking, parametrized saddle-point problems) is ensuring the stability of the resulting RB problem. This is the main reason why, for instance, reduced-order models for fluid dynamics problems have sometimes focused on approximations for the velocity field uniquely, recovering then the pressure in a different way, rather than building a reduced-order approximation based on a mixed velocity-pressure formulation, [12]. Indeed, it is well-known that in the FE case an *inf-sup* condition must be satisfied at the finite dimensional level to ensure the well-posedness of the numerical problem. This condition is fulfilled if either $\mathbb{P}^2-\mathbb{P}^1$ (Taylor-Hood) couples of FE spaces are used for discretizing the velocity and pressure fields, respectively or a stabilized FE formulation is employed, e.g. by relying on the streamline-upwind Petrov-Galerkin (SUPG) method. Hereon we rely on the former option for the high-fidelity FE problem, see e.g. [33, 29] for further details about the latter. Concerning the stability of the RB approximation, a stable couple of reduced subspaces for velocity and pressure, satisfying an equivalent *inf-sup* condition at the reduced level, ensures that the RB Stokes

[1]For example, we can regard the proposed strategy as a step towards the efficient reduction of parametrized fluid-structure interaction problems, where the deformation of the domain is computed through a structural problem coupled with the fluid equations.

problem is well-posed. This property is not automatically fulfilled if the RB problem is constructed through a Galerkin projection employing RB spaces made solely of orthonormalized solutions of (1) obtained for different values of parameters. Two overcome this shortcoming, two strategies have been designed.

A. The velocity space can be augmented by means of a set of *enriching* basis functions computed through the pressure supremizing operator, which depends on the divergence term. This yields a RB problem with additional degrees of freedom for the velocity field (as many as the pressure variable), see [38] for the details. In presence of parameter-dependent domains, the supremizing operator is $\boldsymbol{\mu}$-dependent, so that to recover computational efficiency (and avoid the construction of the pressure supremizing operator for any value of $\boldsymbol{\mu}$ online), an offline enrichment is employed. This strategy leads to a RB problem which is *inf-sup* stable in practice, but its well-posedness is not proven rigorously. Such a framework has been originally introduced in conjunction with a (weak) greedy algorithm [39, 23, 38], and later for the POD case. In the former case, for each pressure basis selected by the greedy algorithm, a supremizing function is used to augment the velocity space. In the latter case, however, the basis functions are not directly related to any precise instance of the parameter, so that a set of enriching functions for the velocity space must be computed in advance starting from the pressure snapshots, then POD is applied to build the enriching basis [4]. This technique allows to build a stable RB problem, however it is not clear, a priori, how many supremizing functions are needed to properly stabilize the problem. Taking as many enriching functions as the number of velocity and pressure basis is a working rule of thumb, however very likely this leads to an excessive number of basis functions.

B. We can exploit a Petrov-Galerkin (PG) method [1, 33] to build an automatically stable RB problem; we choose the least squares (LS) method. The resulting LS-RB method relies on a test space which is obtained as the image of the RB space through a global supremizing operator involving both velocity and pressure fields. The corresponding algebraic construction of this operator substantially relies on the choice of the matrix-norm to be used for the velocity and pressure spaces. By this approach the resulting RB problem is automatically stable – that is, it satisfies the required *inf-sup* condition – as usually happens when dealing with PG-RB methods for weakly coercive problems, see [33] for further details. However, the existing formulation of the LS-RB method for Stokes equations proposed in [1] presumes the existence of an explicit $\boldsymbol{\mu}-$dependent function which enables to recast the problem on a reference domain. Without this function available, as in the case where the deformation results from the solution of a FE problem, the computational work to build the RB problem is unbearable.

In this work we propose a new, purely algebraic, PG-RB method to address large-scale parametrized Stokes equations in domains with varying geometry. Our method can be seen as an algebraic LS-RB method; for this reason we refer to it as aLS-RB method. The aLS-RB method extends and improves the existing RB methods for Stokes equations in several directions, potentially becoming a paradigm for the *efficient* construction of a *stable* and *accurate* RB method for Stokes equations and, more generally speaking, weakly coercive problems. Indeed:

1. it relies on POD – rather than on a greedy algorithm for the construction of the RB spaces for velocity and pressure, thus avoiding the evaluation of potentially expensive a posteriori error bounds; however, like in the greedy case, an exponential decay of the residuals with respect to N is obtained;
2. it does not need an enrichment of the velocity space, by relying on a Petrov-Galerkin method;
3. it exploits suitable approximations of the matrix-norm in the definition of the supremizing operator;
4. the resulting aLS-RB problem rigorously is *inf-sup* stable;
5. it does not require any analytical map between a reference domain and the physical domain $\Omega^{\boldsymbol{\mu}}$;
6. it provides a fully automated procedure to assemble and solve the RB problem, able to treat any kind of parametrization.

To enhance the efficiency of the resulting RB methods, we employ the discrete empirical interpolation method (DEIM) [5, 15], and the Matrix DEIM (M-DEIM) [30] to find an affine approximation of the (generally nonaffine) right hand sides and matrices of the high-fidelity system. We analyze the well-posedness of the aLS-RB method and prove that under suitable conditions it satisfies an *inf-sup* stable RB approximation. A numerical comparison between the proposed aLS-RB method and the current state-of-art G-RB method relying on the enriched velocity space, shows that the former approach is cheaper, both during the offline phase, since the velocity enriching snapshots must not be computed, and the online phase, due to the generally smaller dimension of the resulting RB problem.

We apply the aLS-RB method to solve the three-dimensional Stokes system defined over parameter-dependent domains, with up to millions of degrees of freedom for the high fidelity solution, for which the mapping from a reference domain is not necessarily known analytically. For the case at hand, we consider a geometry which is parametrized with respect to the deformation obtained by solving an elliptic PDE problem which harmonically extends some Dirichlet data, playing the role of imposed shape deformation.

The paper breaks down as follows. In Section 2 we briefly recall the Stokes equations and their FE approximation. In Section 3 we introduce the POD-RB method, with particular emphasis on how to construct a stable RB method either using a Galerkin or Petrov Galerkin projection. Then, we present the aLS-RB and its analysis. In Section 4 we present numerical results obtained with the different RB approximations and in Section 5 we draw some conclusions. Concerning notation, hereon we denote scalar fields by lower case letters, as $a \in \mathbb{R}$, vector fields with an arrow, as $\vec{a} \in \mathbb{R}^d$, for $d = 2, 3$, vectors (like finite elements vectors) by bold lower case letters, as $\mathbf{a} \in \mathbb{R}^n$, and matrices by bold capital letters, as $\mathbf{A} \in \mathbb{R}^{n \times n}$. We denote by $(\cdot,\cdot)_2$ the Euclidean scalar product and by $\mathcal{K}_2(\mathbf{A})$ the condition number of the matrix $\mathbf{A}$ with respect the Euclidean norm. Moreover, given a symmetric and positive definite matrix $\mathbf{Y} \in \mathbb{R}^{n \times n}$, we denote by $(\cdot,\cdot)_{\mathbf{Y}}$ the scalar product and by $\|\cdot\|_{\mathbf{Y}}$ the norm defined as $(\mathbf{a},\mathbf{b})_{\mathbf{Y}} = \mathbf{a}^T\mathbf{Y}\mathbf{b}\ \forall \mathbf{a}, \mathbf{b} \in \mathbb{R}^n$ and $\|\mathbf{a}\|_{\mathbf{Y}} = \sqrt{(\mathbf{a},\mathbf{a})_{\mathbf{Y}}}\ \forall \mathbf{a} \in \mathbb{R}^n$, respectively. Finally, we denote by $\mathcal{K}_{\mathbf{Y}}(\mathbf{A})$ the condition number of $\mathbf{A}$ with respect to the norm $\|\cdot\|_{\mathbf{Y}}$.

2 Parametrized Stokes equations: setting and preliminaries

In this section we introduce the Stokes equations in parametrized domains, together with their weak formulation and a corresponding FE approximation. Denote by $\mathcal{D} \subset \mathbb{R}^l$, $l \in \mathbb{N}$ the parameter space and by $\boldsymbol{\mu} \in \mathcal{D}$ a vector of parameters encoding physical and/or geometrical properties. Heron, the apex $\boldsymbol{\mu}$ means that a variable depends on the specific choice of the parameter $\boldsymbol{\mu}$. Given a $\boldsymbol{\mu}-$dependent domain $\Omega^{\boldsymbol{\mu}} \subset \mathbb{R}^d$, $d = 2$, 3, such that, for any $\boldsymbol{\mu} \in \mathcal{D}$, $\partial\Omega^{\boldsymbol{\mu}} = \Gamma^{\boldsymbol{\mu}}_{out} \cup \Gamma^{\boldsymbol{\mu}}_{in} \cup \Gamma^{\boldsymbol{\mu}}_{w}$ and $\mathring{\Gamma}^{\boldsymbol{\mu}}_{out} \cap \mathring{\Gamma}^{\boldsymbol{\mu}}_{in} = \mathring{\Gamma}^{\boldsymbol{\mu}}_{w} \cap \mathring{\Gamma}^{\boldsymbol{\mu}}_{in} = \mathring{\Gamma}^{\boldsymbol{\mu}}_{out} \cap \mathring{\Gamma}^{\boldsymbol{\mu}}_{w} = \emptyset$, the Stokes equations read

$$\begin{cases} -\nu^{\boldsymbol{\mu}}\Delta\vec{u}^{\boldsymbol{\mu}} + \nabla p^{\boldsymbol{\mu}} = \vec{f}^{\boldsymbol{\mu}} & \text{in } \Omega^{\boldsymbol{\mu}} \\ \nabla \cdot \vec{u}^{\boldsymbol{\mu}} = 0 & \text{in } \Omega^{\boldsymbol{\mu}} \\ \vec{u} = \vec{g}^{\boldsymbol{\mu}}_D & \text{on } \Gamma^{\boldsymbol{\mu}}_{in} \\ \vec{u} = \vec{0} & \text{on } \Gamma^{\boldsymbol{\mu}}_{w} \\ -p^{\boldsymbol{\mu}}\vec{n}^{\boldsymbol{\mu}} + \nu^{\boldsymbol{\mu}}\frac{\partial\vec{u}^{\boldsymbol{\mu}}}{\partial\vec{n}^{\boldsymbol{\mu}}} = \vec{g}^{\boldsymbol{\mu}}_N & \text{on } \Gamma^{\boldsymbol{\mu}}_{out}, \end{cases} \tag{2}$$

where $(\vec{u}^{\boldsymbol{\mu}}, p^{\boldsymbol{\mu}})$ are the velocity and pressure fields of a viscous incompressible Newtonian fluid with viscosity $\nu^{\boldsymbol{\mu}}$, respectively. We introduce a regular enough lifting function $\vec{r}^{\boldsymbol{\mu}}_{\vec{g}_D} \in \left(H^1(\Omega^{\boldsymbol{\mu}})\right)^d$ and the following $\boldsymbol{\mu}$-dependent spaces

$$V^{\boldsymbol{\mu}} = \left\{\vec{v} \in \left(H^1(\Omega^{\boldsymbol{\mu}})\right)^d : \vec{v}\big|_{\Gamma^{\boldsymbol{\mu}}_w} = \vec{v}\big|_{\Gamma^{\boldsymbol{\mu}}_{in}} = \vec{0}\right\},$$
$$Q^{\boldsymbol{\mu}} = L^2(\Omega^{\boldsymbol{\mu}}) \quad \text{or} \quad Q^{\boldsymbol{\mu}} = L^2_0(\Omega^{\boldsymbol{\mu}}) \text{ if } \Gamma^{\boldsymbol{\mu}}_{out} = \emptyset,$$

equipped with scalar products (and corresponding induced norms) $(\cdot,\cdot)_{V^{\boldsymbol{\mu}}} = (\cdot,\cdot)_{(H^1_0(\Omega^{\boldsymbol{\mu}}))^d}$ and $(\cdot,\cdot)_{Q^{\boldsymbol{\mu}}} = (\cdot,\cdot)_{L^2(\Omega^{\boldsymbol{\mu}})}$. For a given $\boldsymbol{\mu} \in \mathcal{D}$, the weak formulation of problem (2) reads: find $(\vec{u}^{\boldsymbol{\mu}}, p^{\boldsymbol{\mu}}) \in V^{\boldsymbol{\mu}} \times Q^{\boldsymbol{\mu}}$ such that

$$\begin{cases} a^{\boldsymbol{\mu}}(\vec{u}^{\boldsymbol{\mu}}, \vec{v}) + b^{\boldsymbol{\mu}}(\vec{v}, p^{\boldsymbol{\mu}}) = f^{\boldsymbol{\mu}}(\vec{v}) & \forall \vec{v} \in V^{\boldsymbol{\mu}} \\ b^{\boldsymbol{\mu}}(\vec{u}^{\boldsymbol{\mu}}, q) = -b^{\boldsymbol{\mu}}(\vec{r}^{\boldsymbol{\mu}}_{\vec{g}_D}, q) & \forall q \in Q^{\boldsymbol{\mu}}, \end{cases} \tag{3}$$

where we define the forms in (3) for $\vec{u}, \vec{v} \in V^{\boldsymbol{\mu}}$, $q \in Q^{\boldsymbol{\mu}}$

$$a^{\boldsymbol{\mu}}(\vec{u}, \vec{v}) = \int_{\Omega^{\boldsymbol{\mu}}} \nu^{\boldsymbol{\mu}} \nabla\vec{u} : \nabla\vec{v} d\Omega^{\boldsymbol{\mu}},$$
$$b^{\boldsymbol{\mu}}(\vec{v}, q) = -\int_{\Omega^{\boldsymbol{\mu}}} q \nabla \cdot \vec{v} d\Omega^{\boldsymbol{\mu}}$$
$$f^{\boldsymbol{\mu}}(\vec{v}) = \int_{\Omega^{\boldsymbol{\mu}}} \vec{f}^{\boldsymbol{\mu}} \cdot \vec{v} d\Omega^{\boldsymbol{\mu}} + \int_{\Gamma^{\boldsymbol{\mu}}_{out}} \vec{g}^{\boldsymbol{\mu}}_N \cdot \vec{v} d\Gamma^{\boldsymbol{\mu}}_{out} - a^{\boldsymbol{\mu}}(\vec{r}^{\boldsymbol{\mu}}_{\vec{g}_D}, \vec{v}).$$

Problem (3) can be written as a symmetric non-coercive problem, provided we define the space $X^{\boldsymbol{\mu}} = V^{\boldsymbol{\mu}} \times Q^{\boldsymbol{\mu}}$, equipped with the scalar product

$$((\vec{u},p),(\vec{v},q))_{X^{\boldsymbol{\mu}}} = (\vec{u},\vec{v})_{V^{\boldsymbol{\mu}}} + (p,q)_{Q^{\boldsymbol{\mu}}}, \qquad (\vec{u},p),(\vec{v},q) \in X^{\boldsymbol{\mu}},$$

and the norm

$$\|(\vec{v},q)\|_{X^{\boldsymbol{\mu}}} = \sqrt{((\vec{v},q),(\vec{v},q))_{X^{\boldsymbol{\mu}}}}, \qquad (\vec{v},q) \in X^{\boldsymbol{\mu}}.$$

Next, we introduce the forms $\mathcal{A}^{\boldsymbol{\mu}} : X^{\boldsymbol{\mu}} \times X^{\boldsymbol{\mu}} \to \mathbb{R}$, $\mathcal{F}^{\boldsymbol{\mu}} : X^{\boldsymbol{\mu}} \to \mathbb{R}$ given by

$$\begin{aligned}\mathcal{A}^{\boldsymbol{\mu}}((\vec{u}^{\boldsymbol{\mu}},p^{\boldsymbol{\mu}}),(\vec{v},q)) &= a^{\boldsymbol{\mu}}(\vec{u},\vec{v}) + b^{\boldsymbol{\mu}}(\vec{v},p^{\boldsymbol{\mu}}) + b^{\boldsymbol{\mu}}(\vec{u}^{\boldsymbol{\mu}},q)\\ \mathcal{F}^{\boldsymbol{\mu}}((\vec{v},q)) &= f^{\boldsymbol{\mu}}(\vec{v}) - b^{\boldsymbol{\mu}}(\vec{r}^{\boldsymbol{\mu}}_{\vec{g}_D},q).\end{aligned}$$

System (3) can thus be equivalently written as: find $\vec{z}^{\boldsymbol{\mu}} \in X^{\boldsymbol{\mu}}$ such that

$$\mathcal{A}^{\boldsymbol{\mu}}(\vec{z}^{\boldsymbol{\mu}},\vec{w}) = \mathcal{F}^{\boldsymbol{\mu}}(\vec{w}) \qquad \forall \vec{w} \in X^{\boldsymbol{\mu}}. \tag{4}$$

The well-posedness of problem (4) is ensured according to the general theory of saddle-point problems [10, 11].

2.1 Finite element approximation of the Stokes equations

Numerical methods based on (Petrov-)Galerkin projection onto a finite dimensional subspace, as the finite element (FE) or spectral element methods, represent a successful technique to handle the numerical approximation of (2), see e.g. [13, 21, 35]. However, when they are employed, a discrete *inf-sup* condition must be satisfied to ensure the well-posedness of the numerical problem.

All the reduced order models considered in this paper for the efficient solution of the parametrized problem (4) hinge upon a high-fidelity finite element approximation, which we introduce in this section. We consider a domain deformation dependent on $\boldsymbol{\mu}$; the corresponding meshes are also taken as a deformation of a reference mesh, hence not affecting the topology of the degrees of freedom. In this work, we do not focus on $h-$refinement, therefore we consider a fixed regular mesh which is fine enough for the problem at hand.

Let us denote by $V_h^{\boldsymbol{\mu}}$ and $Q_h^{\boldsymbol{\mu}}$ two finite dimensional FE spaces of dimension N_h^u and N_h^p, respectively, with $V_h^{\boldsymbol{\mu}} \subset V$ and $Q_h^{\boldsymbol{\mu}} \subset Q$. Moreover, set $X_h^{\boldsymbol{\mu}} = V_h^{\boldsymbol{\mu}} \times Q_h^{\boldsymbol{\mu}}$ with dimension $N_h = N_h^u + N_h^p$. The FE approximation of problem (4) reads: find $\vec{z}_h^{\boldsymbol{\mu}} \in X_h^{\boldsymbol{\mu}}$ such that

$$\mathcal{A}^{\boldsymbol{\mu}}(\vec{z}_h^{\boldsymbol{\mu}},\vec{w}_h) = \mathcal{F}^{\boldsymbol{\mu}}(\vec{w}_h) \qquad \forall \vec{w}_h \in X_h^{\boldsymbol{\mu}}. \tag{5}$$

We further assume that the following $\boldsymbol{\mu}-$uniform *inf-sup* condition holds: there exists a positive constant $\beta^{min} > 0$, independent of $\boldsymbol{\mu}$, such that

$$\beta_h^{\boldsymbol{\mu}} = \inf_{\vec{z}_h \in X_h^{\boldsymbol{\mu}}} \sup_{\vec{w}_h \in X_h^{\boldsymbol{\mu}}} \frac{\mathcal{A}^{\boldsymbol{\mu}}(\vec{z}_h,\vec{w}_h)}{\|\vec{z}_h\|_{X^{\boldsymbol{\mu}}}\|\vec{w}_h\|_{X^{\boldsymbol{\mu}}}} \geq \beta^{min} \qquad \forall \boldsymbol{\mu} \in \mathcal{D}. \tag{6}$$

A couple of FE spaces which fulfills condition (6) is given by $\mathbb{P}^2 - \mathbb{P}^1$ (Taylor-Hood) finite elements, for velocity and pressure, respectively. Condition (6) ensures the stability of problem (5). Problem (5) can be equivalently written as a parametrized linear system

$$\mathbf{A}_h^{\boldsymbol{\mu}}\mathbf{z}_h^{\boldsymbol{\mu}} = \mathbf{g}_h^{\boldsymbol{\mu}}, \tag{7}$$

featuring a saddle-point structure, where

$$\mathbf{A}_h^{\boldsymbol{\mu}} = \begin{bmatrix}\mathbf{D}_h^{\boldsymbol{\mu}} & (\mathbf{B}_h^{\boldsymbol{\mu}})^T\\ \mathbf{B}_h^{\boldsymbol{\mu}} & 0\end{bmatrix}, \qquad \mathbf{z}_h^{\boldsymbol{\mu}} = \begin{bmatrix}\mathbf{u}_h^{\boldsymbol{\mu}}\\ \mathbf{p}_h^{\boldsymbol{\mu}}\end{bmatrix} \qquad \text{and} \qquad \mathbf{g}_h^{\boldsymbol{\mu}} = \begin{bmatrix}\mathbf{f}_h^{\boldsymbol{\mu}}\\ \mathbf{r}_h^{\boldsymbol{\mu}}\end{bmatrix}, \tag{8}$$

where $\mathbf{A}_h^{\boldsymbol{\mu}} \in \mathbb{R}^{N_h \times N_h}$ and $\mathbf{z}_h^{\boldsymbol{\mu}}, \mathbf{g}_h^{\boldsymbol{\mu}} \in \mathbb{R}^{N_h}$. More precisely $\mathbf{D}_h^{\boldsymbol{\mu}} \in \mathbb{R}^{N_h^u \times N_h^u}$, $\mathbf{B}_h^{\boldsymbol{\mu}} \in \mathbb{R}^{N_h^p \times N_h^u}$, $\mathbf{f}_h^{\boldsymbol{\mu}} \in \mathbb{R}^{N_h^u}$ and finally $\mathbf{r}_h^{\boldsymbol{\mu}} \in \mathbb{R}^{N_h^p}$. The solution of system (7) exploits suitable iterative methods properly preconditioned. Several techniques relying on domain decomposition, multilevel methods and block factorizations have been proposed as preconditioners, see e.g. [21, 32, 40, 36] and references therein. See also [6, 7] for an extensive review on numerical methods for saddle-point systems.

Condition (6) can be algebraically expressed as follows: there exists $\beta^{min} > 0$ such that

$$\beta_h^{\boldsymbol{\mu}} = \inf_{\vec{z}_h \in \mathbb{R}^{N_h}} \sup_{\vec{w}_h \in \mathbb{R}^{N_h}} \frac{\mathbf{w}_h^T \mathbf{A}_h^{\boldsymbol{\mu}} \mathbf{z}_h}{\|\mathbf{z}_h\|_{\mathbf{X}_h^{\boldsymbol{\mu}}} \|\mathbf{w}_h\|_{\mathbf{X}_h^{\boldsymbol{\mu}}}} \geq \beta^{min} \qquad \forall \boldsymbol{\mu} \in \mathcal{D}, \tag{9}$$

where the symmetric and positive definite matrix $\mathbf{X}_h^{\boldsymbol{\mu}} \in \mathbb{R}^{N_h \times N_h}$ encodes the scalar product $(\cdot,\cdot)_{X^{\boldsymbol{\mu}}}$ on the space $X_h^{\boldsymbol{\mu}}$ and is built as a block diagonal matrix of the form

$$\mathbf{X}_h^{\boldsymbol{\mu}} = \begin{bmatrix} \mathbf{X}_u^{\boldsymbol{\mu}} & 0 \\ 0 & \mathbf{X}_p^{\boldsymbol{\mu}} \end{bmatrix}; \tag{10}$$

$\mathbf{X}_u^{\boldsymbol{\mu}} \in \mathbb{R}^{N_h^u \times N_h^u}$ and $\mathbf{X}_p^{\boldsymbol{\mu}} \in \mathbb{R}^{N_h^p \times N_h^p}$ encode the scalar products on the spaces $V_h^{\boldsymbol{\mu}}$ and $Q_h^{\boldsymbol{\mu}}$, respectively. Notice that since the computational domain is $\boldsymbol{\mu}-$dependent, also the matrix $\mathbf{X}_h^{\boldsymbol{\mu}}$ depends on the parameter $\boldsymbol{\mu}$.

3 POD-based RB methods for the parametrized Stokes equations

The RB method represents a convenient framework for the reduction of parametrized PDEs [33, 24]. Such a method essentially combines a technique to generate a low-dimensional subspace of $X_h^{\boldsymbol{\mu}}$ where the RB solution is sought, and a Galerkin-type projection (either Galerkin or Petrov-Galerkin) onto the subspace to obtain the corresponding RB problem to be solved. Here we rely upon proper orthogonal decomposition (POD) because we do not have a cheaply computable a-posteriori error bound, which would instead be required if a greedy algorithm were performed. Then, a new algebraic PG-RB method is investigated for the sake of the construction of the RB problem, and compared to the (indeed, more classical) Galerkin-RB method which relies on properly enriched RB spaces. In the following, we recall the essential elements of this technique and how it is used to build a RB approximation.

3.1 Constructing the RB space: proper orthogonal decomposition

Let us consider a set of n_s FE vectors $\{\mathbf{s}_i\}_{i=1}^{n_s} \subset \mathbb{R}^{N_h}$ (called *snapshots*) collected as columns of a matrix $\mathbf{S} = [\mathbf{s}_1| \dots |\mathbf{s}_{n_s}]$, $\mathbf{S} \in \mathbb{R}^{N_h \times n_s}$. For any prescribed dimension N, the POD allows to find an orthonormal basis $\{\boldsymbol{\xi}_i\}_{i=1}^{n_s}$ and the corresponding N-dimensional subspace, spanned by the columns of the matrix $\mathbf{V} = [\boldsymbol{\xi}_1| \dots |\boldsymbol{\xi}_N]$, $\mathbf{V} \in \mathbb{R}^{N_h \times N}$ which best approximates $\{\mathbf{s}_i\}_{i=1}^{n_s}$ up to a tolerance ε_{POD} with respect to a prescribed norm induced by a symmetric positive definite matrix $\mathbf{X} \in \mathbb{R}^{N_h \times N_h}$. The POD method takes advantage of the singular value decomposition (SVD) of the matrix $\mathbf{S}$

$$\mathbf{S} = \mathbf{U}\boldsymbol{\Sigma}\mathbf{Z}^T,$$

with $\mathbf{U} \in \mathbb{R}^{N_h \times N_h}$ and $\mathbf{Z} \in \mathbb{R}^{n_s \times n_s}$ orthogonal matrices and $\boldsymbol{\Sigma} = diag(\sigma_1, \dots \sigma_{n_s})$, $\boldsymbol{\Sigma} \in \mathbb{R}^{N_h \times n_s}$, containing the singular values $\sigma_1 \geq \sigma_2 \geq \cdots \geq \sigma_{n_s} \geq 0$. Then, $\mathbf{V}$ is provided by the first N columns of $\mathbf{U}$, which form by construction an orthonormal basis for the best N-dimensional approximation subspace. More in particular, denoting $\mathbf{I}_N \in \mathbb{R}^{N \times N}$ the N-dimensional identity matrix, the following proposition holds [33].

Proposition 3.1. *Let $\mathcal{V}_N = \{\mathbf{W} \in \mathbb{R}^{N_h \times N} : \mathbf{W}^T\mathbf{X}_h\mathbf{W} = \mathbf{I}_N\}$ be the set of all N-dimensional* **X**-*orthonormal bases. Then*

$$\sum_{i=1}^{n_s} \|\mathbf{s}_i - \mathbf{V}\mathbf{V}^T\mathbf{X}\mathbf{s}_i\|_{\mathbf{X}}^2 = \min_{\mathbf{W} \in \mathcal{V}_N} \sum_{i=1}^{n_s} \|\mathbf{s}_i - \mathbf{W}\mathbf{W}^T\mathbf{X}\mathbf{s}_i\|_{\mathbf{X}}^2 = \sum_{i=N+1}^{n_s} \sigma_i^2.$$

Moreover, notice that the relative error on all the snapshots is related to $\{\sigma_i\}_i^{n_s}$ through the following relation

$$\frac{\sum_{i=1}^{n_s} \|\mathbf{s}_i - \mathbf{V}\mathbf{V}^T\mathbf{X}\mathbf{s}_i\|_{\mathbf{X}}^2}{\sum_{i=1}^{n_s} \|\mathbf{s}_i\|_{\mathbf{X}}^2} = \frac{\sum_{i=N+1}^{n_s} \sigma_i^2}{\sum_{i=1}^{n_s} \sigma_i^2}. \tag{11}$$

From a practical perspective, the POD basis construction is done following Algorithm 1. At first the correlation matrix $\mathbf{C}_{n_s} = \mathbf{S}^T\mathbf{X}\mathbf{S}$ is formed and the corresponding eigenvalue problem is solved. Then, for a given tolerance ε_{POD}, (11) is employed to control the relative error on the approximation of the snapshots and select N basis functions. Alternatively, one could directly provide a dimension N instead of ε_{POD}, leading to a similar algorithm POD($\mathbf{S}$, $\mathbf{X}$, N).

Algorithm 1 POD

procedure POD($\mathbf{S}$, $\mathbf{X}$, ε_{POD})
  form the correlation matrix $\mathbf{C}_{n_s} = \mathbf{S}^T\mathbf{X}\mathbf{S}$
  solve the eigenvalue problem $\mathbf{C}_{n_s}\boldsymbol{\psi_i} = \sigma_i^2\boldsymbol{\psi_i}, \quad i = 1, \ldots, n_s$
  set $\boldsymbol{\xi}_i = \frac{1}{\sigma_i}\mathbf{S}\boldsymbol{\psi_i}$
  define N as the minimum integer such that $\frac{\sum_{i=1}^{N}\sigma_i^2}{\sum_{i=1}^{n_s}\sigma_i^2} > 1 - \varepsilon_{\text{POD}}^2$
  define $\mathbf{V} = [\boldsymbol{\xi}_1|\ldots|\boldsymbol{\xi}_N]$
end procedure

3.2 Projection-based RB methods

The RB method relies on the idea that the solution of the parametrized system (7), for a certain value of the parameter $\boldsymbol{\mu}$, can be well approximated by a linear combination of N basis functions $\{\vec{\xi}_i\}_{i=1}^N$ obtained by orthonormalizing the solutions of the same problem for other values of the parameter. The basis functions are collected in the so-called RB space, which is defined as

$$V_N = span\{\vec{\xi}_i,\, i = 1, \ldots, N\} \tag{12}$$

of dimension $N \ll N_h$. From an algebraic standpoint V_N is represented by the matrix $\mathbf{V} = [\boldsymbol{\xi}_1|\ldots|\boldsymbol{\xi}_N] \in \mathbb{R}^{N_h \times N}$, where $\boldsymbol{\xi}_i, i = 1, \ldots, N$ are the FE vector representation of the basis $\vec{\xi}_i, i = 1, \ldots, N$. From a practical standpoint, the vector basis $\{\boldsymbol{\xi}_i\}_{i=1}^N$ is constructed by exploiting POD where the snapshots are FE solutions of the FE linear system for many instances of the parameter, i.e. $\mathbf{s}_i = \mathbf{z}_h^{\boldsymbol{\mu}_i}$, $i = 1, \ldots, n_s$ Then, the RB approximation is constructed by introducing a set of (possibly $\boldsymbol{\mu}-$dependent) functions $\{w_i^{\boldsymbol{\mu}}\}_{i=1}^N$ such that a test space $W_N^{\boldsymbol{\mu}}$ is obtained as

$$W_N^{\boldsymbol{\mu}} = span\{w_i^{\boldsymbol{\mu}},\, i = 1, \ldots, N\}.$$

Algebraically, $W_N^{\boldsymbol{\mu}}$ is represented by a matrix $\mathbf{W}^{\boldsymbol{\mu}} \in \mathbb{R}^{N_h \times N}$, which is generally different from $\mathbf{V}$ and may be $\boldsymbol{\mu}$-dependent. If $\mathbf{W}^{\boldsymbol{\mu}} \neq \mathbf{V}$ we have the more general Pevtrov Galerkin-RB approximation, otherwise if $\mathbf{W}^{\boldsymbol{\mu}} = \mathbf{V}$ we come up with the usual Galerkin case. For the sake of generality, we consider the PG-RB problem, which reads: find $\vec{z}_N^{\boldsymbol{\mu}} \in V_N$ such that

$$\mathcal{A}^{\boldsymbol{\mu}}(\vec{z}_N^{\boldsymbol{\mu}}, \vec{w}_N) = \mathcal{F}^{\boldsymbol{\mu}}(\vec{w}_N) \qquad \forall \vec{w}_N \in W_N^{\boldsymbol{\mu}}. \tag{13}$$

In order to obtain a well-posed RB approximation, an *inf-sup* condition at the RB level must also be satisfied. Specifically, there must exist $\beta_N^{min} > 0$ independent of $\boldsymbol{\mu}$ such that

$$\beta_N^{\boldsymbol{\mu}} = \inf_{\vec{z}_N \in V_N} \sup_{\vec{w}_N \in W_N^{\boldsymbol{\mu}}} \frac{\mathcal{A}^{\boldsymbol{\mu}}(\vec{z}_N, \vec{w}_N)}{\|\vec{z}_N\|_{X^{\mu}}\|\vec{w}_N\|_{X^{\mu}}} \geq \beta_N^{min} > 0 \qquad \forall \boldsymbol{\mu} \in \mathcal{D}. \tag{14}$$

Ensuring this condition, as we will see in the following, essentially depends on the type of projection used to generate the RB problem and the way the RB spaces are built. Problem (13) leads to the following algebraic RB linear system

$$\mathbf{A}_N^{\boldsymbol{\mu}}\mathbf{z}_N^{\boldsymbol{\mu}} = \mathbf{g}_N^{\boldsymbol{\mu}}, \tag{15}$$

where the RB matrix $\mathbf{A}_N^{\boldsymbol{\mu}} \in \mathbb{R}^{N \times N}$ and the RB right hand side $\mathbf{g}_N^{\boldsymbol{\mu}} \in \mathbb{R}^N$ are defined as

$$\mathbf{A}_N^{\boldsymbol{\mu}} = (\mathbf{W}^{\boldsymbol{\mu}})^T\mathbf{A}_h^{\boldsymbol{\mu}}\mathbf{V}, \qquad \mathbf{g}_N^{\boldsymbol{\mu}} = (\mathbf{W}^{\boldsymbol{\mu}})^T\mathbf{g}_h^{\boldsymbol{\mu}}. \tag{16}$$

We highlight that the PG-RB approximation depends on the choice of the test space $W_N^{\boldsymbol{\mu}}$. As remarked above, the matrix $\mathbf{V}$ is built employing the POD method, which in the Stokes case turns to

$$\mathbf{V} = \begin{bmatrix} \mathbf{V}_{N_u}^u & 0 \\ 0 & \mathbf{V}_{N_p}^p \end{bmatrix} = \left[\boldsymbol{\xi}_1|\ldots|\boldsymbol{\xi}_{N_u}|\boldsymbol{\xi}_{N_u+1}|\ldots|\boldsymbol{\xi}_N\right], \tag{17}$$

where $\mathbf{V}_{N_u}^u \in \mathbb{R}^{N_h^u \times N_u}$ and $\mathbf{V}_{N_p}^p \in \mathbb{R}^{N_h^p \times N_p}$ are the basis to approximate the velocity $\mathbf{u}_h^{\boldsymbol{\mu}}$ and the pressure $\mathbf{p}_h^{\boldsymbol{\mu}}$, respectively. In particular

$$\boldsymbol{\xi}_i = \begin{bmatrix} \boldsymbol{\varphi}_i \\ \mathbf{0} \end{bmatrix} \quad i = 1, \ldots, N_u, \qquad\qquad \boldsymbol{\xi}_{N_u+i} = \begin{bmatrix} \mathbf{0} \\ \boldsymbol{\psi}_i^p \end{bmatrix} \quad i = 1, \ldots, N_p,$$

where $\{\boldsymbol{\varphi}_i\}_i^{N_u}$ and $\{\boldsymbol{\psi}_i\}_i^{N_p}$ are the basis functions for the velocity and the pressure RB space, that is,

$$\mathbf{V}_{N_u}^u = [\boldsymbol{\varphi}_1^u|\dots|\boldsymbol{\varphi}_{N_u}], \qquad \mathbf{V}_{N_p}^p = [\boldsymbol{\psi}_1|\dots|\boldsymbol{\psi}_{N_p}].$$

The construction of the RB spaces is thus performed by first collecting a set of FE snapshots $\{\mathbf{u}_h^{\boldsymbol{\mu}_i}\}_{i=1}^{n_s}$, $\{\mathbf{p}_h^{\boldsymbol{\mu}_i}\}_{i=1}^{n_s}$, solutions of (7) for different instances of the parameters $\{\boldsymbol{\mu}_i\}_{i=1}^{n_s}$, and then performing POD separately on the two spaces

$$\mathbf{V}_{N_u}^u = POD\Big(\mathbf{S}_{\vec{u}}, \mathbf{X}_u, \varepsilon_{\text{POD}}\Big), \qquad \mathbf{V}_{N_p}^p = POD\Big(\mathbf{S}_p, \mathbf{X}_p, \varepsilon_{\text{POD}}\Big).$$

The matrices $\mathbf{V}_{N_u}^u$ and $\mathbf{V}_{N_p}^p$ are constructed by selecting the largest N_u and N_p eigenmodes respectively, as explained in Algorithm 1, finally obtaining $N_u + N_p = N$, see [33]. Notice that a priori $N_u \neq N_p$. The trial reduced basis spaces are defined by considering the sets of basis $\{\vec{\varphi}_i\}_{i=1}^{N_u}$ and $\{\psi_i\}_{i=1}^{N_p}$, whose FE vector representations are given by $\{\boldsymbol{\varphi}_i\}_{i=1}^{N_u}$ and $\{\boldsymbol{\psi}_i\}_{i=1}^{N_p}$. Then, we define

$$V_{N_u} = span\{\vec{\varphi}_i,\, i = 1,\dots,N_u\} \qquad Q_{N_p} = span\{\psi_i,\, i = 1,\dots,N_p\},$$

and $V_N = (V_{N_u}, Q_{N_p})$. We finally remark that the dimension $N = N_u + N_p$ of the RB system is smaller of the dimension N_h of the FE linear system of several orders of magnitude: $N \ll N_h$, so that problem (15) is solved by direct methods.

Several ways to produce a well-posed Stokes RB problem, relying either on Galerkin or Petrov-Galerkin projection, are available. The Galerkin RB approximation relies on a velocity enrichment strategy, where the velocity RB space V_{N_u} is augmented with an additional RB space built through a pressure supremizing operator, as explained e.g. in [4]. This method has been proposed for both POD and greedy RB space construction, and, even if empirically it works properly, it does not rigorously ensure the well-posedness of the resulting RB problem. Furthermore, when using POD it is unclear how large the augmenting space should be.

In the following sections we report both the Galerkin and Petrov-Galerkin RB approximations as well as alternative ways to construct the RB spaces, to deal with the parametrized Stokes equations; in the section of numerical experiments, we will report results using both these techniques.

3.2.1 Galerkin-RB method with velocity enrichment

A Galerkin-RB formulation is obtained by choosing $W_N^{\boldsymbol{\mu}} = V_N$ (or algebraically $\mathbf{W}^{\boldsymbol{\mu}} = \mathbf{V}$) in (16), resulting in a RB approximation whose well-posedness is guaranteed by satisfying the following assumption: there must exist $\tilde{\beta}_N^{min} > 0$ such that

$$\tilde{\beta}_N^{\boldsymbol{\mu}} = \inf_{q_N \in Q_{N_p}} \sup_{\vec{v}_N \in V_{N_u}} \frac{b^{\boldsymbol{\mu}}(\vec{v}_N, q_N)}{\|\vec{v}_N\|_{V^{\boldsymbol{\mu}}} \|q_N\|_{Q^{\boldsymbol{\mu}}}} \geq \tilde{\beta}_N^{min} > 0 \qquad \forall \boldsymbol{\mu} \in \mathcal{D}. \tag{18}$$

Unfortunately, as explained above, condition (18) is not automatically satisfied when the RB spaces V_{N_u} and Q_{N_p} are constructed by POD, or by greedy algorithms, by considering basis functions extracted from velocity and pressure snapshots only. Consequently, we consider an "enriched" velocity space formulation, as proposed in [4], where the velocity space V_{N_u} is augmented to guarantee the well-posedness of the resulting RB approximation. Algebraically, this is pursued by building a matrix $\mathbf{V}_{N_s}^s \in \mathbb{R}^{N_h^u \times N_s}$ whose columns form a basis for the enriching RB velocity space. Then, the G-RB approximation is built by considering $\mathbf{V} = \mathbf{W}^{\boldsymbol{\mu}} = \tilde{\mathbf{V}}$ in (16), where $\tilde{\mathbf{V}}$ is defined as

$$\tilde{\mathbf{V}} = \begin{bmatrix} \mathbf{V}_{N_u}^u & \mathbf{V}_{N_s}^s & 0 \\ 0 & 0 & \mathbf{V}_{N_p}^p \end{bmatrix}.$$

The enriching strategies are based upon the use of the pressure-supremizing operator $T_p^{\boldsymbol{\mu}} : Q_h^{\boldsymbol{\mu}} \to V_h^{\boldsymbol{\mu}}$ such that for any given $q_h \in Q_h^{\boldsymbol{\mu}}$, it yields $T_p^{\boldsymbol{\mu}}(q_h)$ as the solution of the following problem

$$(T_p^{\boldsymbol{\mu}}(q_h), \vec{v}_h)_{V^{\boldsymbol{\mu}}} = b^{\boldsymbol{\mu}}(\vec{v}_h, q_h) \qquad \forall \vec{v}_h \in V_h^{\boldsymbol{\mu}}. \tag{19}$$

Equation (19) corresponds to a FE problem whose algebraic formulation yields the following linear system

$$\mathbf{X}_u^{\boldsymbol{\mu}} \mathbf{t}_p^{\boldsymbol{\mu}}(\mathbf{q}_h) = (\mathbf{B}_h^{\boldsymbol{\mu}})^T \mathbf{q}_h, \tag{20}$$

where $\mathbf{q}_h \in \mathbb{R}^{N_h^p}$ is the FE vector representation of $q_h \in Q_h^{\boldsymbol{\mu}}$. Two strategies have been developed to build a well-posed G-RB approximation for a new parameter $\boldsymbol{\mu}$:

- build for each pressure basis $\{\boldsymbol{\xi}_i\}_{i=N_u+1}^{N}$ the corresponding supremizing functions $\{\mathbf{t}_p^{\boldsymbol{\mu}}(\boldsymbol{\xi}_i)\}_{i=N_u+1}^{N}$ and define

$$\mathbf{V}_{N_s}^s = [\mathbf{t}_p^{\boldsymbol{\mu}}(\boldsymbol{\xi}_{N_u+1})|\dots|\mathbf{t}_p^{\boldsymbol{\mu}}(\boldsymbol{\xi}_{N_u+1})],$$

leading to a RB formulation which by definition satisfies (18). However, in this way the construction of the supremizing enriching functions is not computationally feasible, because it entails (online) the solution of N_p FE linear system for each new value of $\boldsymbol{\mu}$;

- compute a set of supremizing snapshots $\{\mathbf{t}_p^{\boldsymbol{\mu}_i}(\mathbf{p}_h^{\boldsymbol{\mu}_i})\}_{i=1}^{n_s}$ corresponding to the pressure snapshots $\{\mathbf{p}_h^{\boldsymbol{\mu}_i}\}_{i=1}^{n_s}$ through (20), and then build the matrix $\mathbf{V}_{N_s}^s$ through POD

$$\mathbf{V}_{N_s}^s = POD\Big(\{\mathbf{t}_p^{\boldsymbol{\mu}_i}(\mathbf{p}_h^{\boldsymbol{\mu}_i})\}_{i=1}^{n_s}, \mathbf{X}_u, \varepsilon_{\text{POD}}\Big).$$

Notice that this option does not ensure that condition (18) (or any equivalent one) is satisfied. Moreover, the number N_s of basis functions for $\mathbf{V}_{N_s}^s$ is chosen, with a rule of thumb, equal to N_u, doubling the size of the RB velocity space. This looks like a reliable option which yields a stable RB problem for the steady Navier-Stokes equations, see [4].

3.2.2 LS-RB method

Instead of performing a Galerkin projection onto properly enriched RB spaces, the Petrov-Galerkin (PG)-RB method uses a different test space $\mathbf{W}^{\boldsymbol{\mu}}$ and naturally builds an *inf-sup* stable RB problem. The PG-RB method has been firstly analyzed for the affinely parametrized Stokes equations in [1] where the RB space is built upon a greedy algorithm. In this work we deepen the analysis carried out in [1], propose several strategies to make this method computationally efficient and use instead the POD method for the construction of the RB space, which does not need any error estimator. Moreover, we do not assume to have an analytical function which maps the reference domain Ω^0 to the physical domain $\Omega^{\boldsymbol{\mu}}$; the main consequence is that we consider the more general case where recasting the problem on a reference, parameter-independent domain Ω^0 is not possible. We restrict ourselves to the case of PG-RB method built through the least-squares (LS) method, which automatically guarantees to obtain an *inf-sup* stable problem. With this aim, we introduce a different (global) supremizing operator $T^{\boldsymbol{\mu}} : X_h^{\boldsymbol{\mu}} \to X_h^{\boldsymbol{\mu}}$, such that

$$(T^{\boldsymbol{\mu}}(\vec{z}_h), \vec{w}_h)_{X^{\boldsymbol{\mu}}} = \mathcal{A}^{\boldsymbol{\mu}}(\vec{z}_h, \vec{w}_h) \qquad \forall \vec{w}_h \in X_h^{\boldsymbol{\mu}}. \tag{21}$$

With respect to the definition of $T_p^{\boldsymbol{\mu}}$ provided by (19), both the velocity and pressure appear, together with the full Stokes operator at the right hand side. Given $\vec{z}_h \in X_h^{\boldsymbol{\mu}}$, problem (21) is a $\boldsymbol{\mu}-$dependent FE problem which needs to be solved for $T^{\boldsymbol{\mu}}(\vec{z}_h)$. Then, the RB problem reads as (13), where the test space is chosen as

$$W_N^{\boldsymbol{\mu}} = span\{T^{\boldsymbol{\mu}}(\vec{\xi}_i),\ i = 1, \dots, N\},$$

while the trial RB space is chosen as in (12) with the corresponding matrix $\mathbf{V}$ as in (17). From an algebraic standpoint, given $\mathbf{z}_h \in \mathbb{R}^{N_h}$, the supremizing solution $\mathbf{t}^{\mu}(\mathbf{z}_h)$ is obtained by solving the linear system

$$\mathbf{X}_h^{\boldsymbol{\mu}} \mathbf{t}^{\mu}(\mathbf{z}_h) = \mathbf{A}_h^{\boldsymbol{\mu}} \mathbf{z}_h. \tag{22}$$

The projection matrix $\mathbf{W}^{\boldsymbol{\mu}}$, whose columns are supremizers of type (22) and form a basis for the (parameter-dependent) test space, is then given by

$$\mathbf{W}^{\boldsymbol{\mu}} = (\mathbf{X}_h^{\boldsymbol{\mu}})^{-1} \mathbf{A}_h^{\boldsymbol{\mu}} \mathbf{V}, \tag{23}$$

where $\mathbf{X}_h^{\boldsymbol{\mu}}$ is the $\boldsymbol{\mu}-$dependent norm matrix (10). Finally, the linear system (15) representing the LS-RB problem is recovered with

$$\mathbf{A}_N^{\boldsymbol{\mu}} = \mathbf{V}^T (\mathbf{A}_h^{\boldsymbol{\mu}})^T (\mathbf{X}_h^{\boldsymbol{\mu}})^{-1} \mathbf{A}_h^{\boldsymbol{\mu}} \mathbf{V} \qquad \mathbf{g}_N^{\boldsymbol{\mu}} = \mathbf{V}^T (\mathbf{A}_h^{\boldsymbol{\mu}})^T (\mathbf{X}_h^{\boldsymbol{\mu}})^{-1} \mathbf{g}_h^{\boldsymbol{\mu}}. \tag{24}$$

The following results hold, see also [1, 33].

Lemma 3.1. *Assume that condition* (9) *holds and* $\mathbf{W}^{\boldsymbol{\mu}}$ *is taken as in* (23). *Then, the LS-RB problem* (15) *is* $\boldsymbol{\mu}-$*uniformly inf-sup stable, that is, there exists* $\beta^{min} > 0$ *independent of* $\boldsymbol{\mu}$ *such that*

$$\beta_N^{\boldsymbol{\mu}} = \inf_{\mathbf{z}_N \in \mathbb{R}^N} \sup_{\mathbf{w}_N \in \mathbb{R}^N} \frac{\mathbf{w}_N^T \mathbf{A}_N^{\boldsymbol{\mu}} \mathbf{z}_N}{\|\mathbf{V}\mathbf{z}_N\|_{\mathbf{X}_h^{\boldsymbol{\mu}}} \|\mathbf{W}^{\boldsymbol{\mu}} \mathbf{w}_N\|_{\mathbf{X}_h^{\boldsymbol{\mu}}}} \geq \beta^{min} \qquad \forall \boldsymbol{\mu} \in \mathcal{D}.$$

Moreover, it has a unique solution $\mathbf{z}_N^{\boldsymbol{\mu}} \in \mathbb{R}^N$ *for any* $\boldsymbol{\mu} \in \mathcal{D}$*, which satisfies*

$$\|\mathbf{z}_N^{\boldsymbol{\mu}}\|_{\mathbf{X}_h^{\boldsymbol{\mu}}} \leq \frac{1}{\beta_N^{\boldsymbol{\mu}}} \|\mathbf{g}_h^{\boldsymbol{\mu}}\|_{(\mathbf{X}_h^{\boldsymbol{\mu}})^{-1}}.$$

Proof. We report an algebraic variant of the proof of the result shown in [1]. Starting from (22) and the Cauchy-Schwarz inequality

$$\mathbf{w}_h^T \mathbf{A}_h^{\boldsymbol{\mu}} \mathbf{z}_h = \mathbf{w}_h^T \mathbf{X}_h^{\boldsymbol{\mu}} \mathbf{t}^{\mu}(\mathbf{z}_h) \leq \|\mathbf{t}^{\mu}(\mathbf{z}_h)\|_{\mathbf{X}_h^{\boldsymbol{\mu}}} \|\mathbf{w}_h\|_{\mathbf{X}_h^{\boldsymbol{\mu}}} \qquad \forall \mathbf{w}_h \in \mathbb{R}^{N_h},$$

and the equality is reached for $\mathbf{w}_h = \mathbf{t}^{\mu}(\mathbf{z}_h)$. Then, we have

$$\begin{aligned}\beta_N^{\boldsymbol{\mu}} &= \inf_{\vec{z}_N \in \mathbb{R}^N} \sup_{\vec{w}_N \in \mathbb{R}^N} \frac{\mathbf{w}_N^T \mathbf{A}_N^{\boldsymbol{\mu}} \mathbf{z}_N}{\|\mathbf{V}\mathbf{z}_N\|_{\mathbf{X}_h^{\boldsymbol{\mu}}} \|\mathbf{W}^{\boldsymbol{\mu}} \mathbf{w}_N\|_{\mathbf{X}_h^{\boldsymbol{\mu}}}} = \inf_{\mathbf{z}_N \in \mathbb{R}^N} \frac{\|\mathbf{t}^{\mu}(\mathbf{V}\mathbf{z}_N)\|_{\mathbf{X}_h^{\boldsymbol{\mu}}}}{\|\mathbf{V}\mathbf{z}_N\|_{\mathbf{X}_h^{\boldsymbol{\mu}}}} \\ &\geq \inf_{\mathbf{z}_h \in \mathbb{R}^{N_h}} \frac{\|\mathbf{t}^{\mu}(\mathbf{z}_h)\|_{\mathbf{X}_h^{\boldsymbol{\mu}}}}{\|\mathbf{z}_h\|_{\mathbf{X}_h^{\boldsymbol{\mu}}}} \geq \beta^{min}.\end{aligned}$$

The proof is concluded by employing the Babuška theorem for non-coercive problems satisfying an *inf-sup* stability property, see [2]. □

Remark 3.1. *The solution* $\mathbf{z}_N^{\boldsymbol{\mu}} \in \mathbb{R}^N$ *of problem* (15) *solves the following minimization problem*

$$\mathbf{z}_N^{\boldsymbol{\mu}} = \arg \min_{\mathbf{v}_N \in \mathbb{R}^N} \|\mathbf{g}_h^{\boldsymbol{\mu}} - \mathbf{A}_h^{\boldsymbol{\mu}} \mathbf{V} \mathbf{v}_N\|^2_{(\mathbf{X}_h^{\boldsymbol{\mu}})^{-1}}, \tag{25}$$

i.e. the RB solution minimizes the residual in the norm induced by the symmetric positive definite matrix $(\mathbf{X}_h^{\boldsymbol{\mu}})^{-1}$*, see [33] for further details.*

3.3 Algebraic LS-RB method

The LS-RB method described in Section 3.2.2 requires to build the $\boldsymbol{\mu}$-dependent matrix $(\mathbf{X}_h^{\boldsymbol{\mu}})^{-1}$ or to solve approximately the N linear systems (22) associated with the matrix $\mathbf{X}_h^{\boldsymbol{\mu}}$ to construct a stable RB problem for any new parameter instances $\boldsymbol{\mu} \in \mathcal{D}$ considered online. If an analytical map is available, one can recast problem (4) over the reference domain Ω^0 by using the Jacobian of the map. In this way, the LS-RB problem would be built with respect to the reference domain, and the independence of the norm matrix $\mathbf{X}_h^{\boldsymbol{\mu}}$ on $\boldsymbol{\mu}$ would be easily achieved. However, if the displacement of the domain is not analitically available, it is not possible to rely on this strategy. In this section we propose a purely algebraic PG-RB method which can be viewed as an algebraic LS-RB (aLS-RB) method described above for parametrized noncoercive problems as (7). Compared to the approximate enrichment of the velocity space described in section (3.2.1), the aLS-RB method allows to build a RB problem which is automatically and rigorously *inf-sup* stable and henceforth it does not require to enrich the velocity space doubling the degrees of freedom of the velocity.

The underlying idea is to substitute the matrix $\mathbf{X}_h^{\boldsymbol{\mu}}$ appearing in the definition of the test space (23) by a properly chosen surrogate $\mathbf{P}_X \in \mathbb{R}^{N_h \times N_h}$. To this aim, we suppose the following assumption to hold.

Assumption 3.1. *The matrix* $\mathbf{P}_X \in \mathbb{R}^{N_h \times N_h}$ *is symmetric and positive definite and induces a norm* $\|\mathbf{x}\|^2_{\mathbf{P}_X} = (\mathbf{x}, \mathbf{x})_{\mathbf{P}_X} = \mathbf{x}^T \mathbf{P}_X \mathbf{x}$ *for any* $\mathbf{x} \in \mathbb{R}^{N_h}$*. Moreover, there exist two positive constants* c *and* C *independent of* $\boldsymbol{\mu}$ *such that*

$$c\|\mathbf{x}\|_{\mathbf{P}_X} \leq \|\mathbf{x}\|_{\mathbf{X}_h^{\boldsymbol{\mu}}} \leq C\|\mathbf{x}\|_{\mathbf{P}_X} \qquad \forall \mathbf{x} \in \mathbb{R}^{N_h}. \tag{26}$$

Next, we introduce a slightly modified supremizing operator $T_{\mathbf{P}_X}^{\boldsymbol{\mu}} : V_h^{\boldsymbol{\mu}} \times V_h^{\boldsymbol{\mu}} \to V_h^{\boldsymbol{\mu}}$ defined by the following problem

$$(T_{\mathbf{P}_X}^{\boldsymbol{\mu}}(\vec{z}_h), \vec{w}_h)_{\mathbf{P}_X} = \mathcal{A}^{\boldsymbol{\mu}}(\vec{z}_h, \vec{w}_h) \qquad \forall \vec{w}_h \in V_h^{\boldsymbol{\mu}}, \tag{27}$$

where the difference with respect to (21) is the choice of the scalar product with respect to which the operator is built. Reasoning as in the previous section, we introduce a PG problem under the form: find $\vec{z}_N \in V_N$ such that

$$\mathcal{A}^{\boldsymbol{\mu}}(\vec{z}_N, \vec{w}_N) = \mathcal{F}^{\boldsymbol{\mu}}(\vec{w}_N) \qquad \forall \vec{w}_N \in W_{N,\mathbf{P}_X}^{\boldsymbol{\mu}}, \tag{28}$$

where now the test space is chosen as

$$W_{N,\mathbf{P}_X}^{\boldsymbol{\mu}} = span\{T_{\mathbf{P}_X}^{\boldsymbol{\mu}}(\vec{\xi}_i),\ i = 1, \ldots, N\},$$

where $\{\vec{\xi}_i\}_{i=1}^N$ are the RB functions defining V_N in (12). Problem (27) is algebraically equivalent to solving

$$\mathbf{P}_X \mathbf{t}^{\mu}_{\mathbf{P}_X}(\mathbf{z}_h) = \mathbf{A}_h \mathbf{z}_h, \tag{29}$$

and yields a projection matrix of the following form

$$\mathbf{W}^{\boldsymbol{\mu}}_{\mathbf{P}_X} = \mathbf{P}_X^{-1}\mathbf{A}_h^{\boldsymbol{\mu}}\mathbf{V}. \tag{30}$$

Finally, the corresponding RB system is

$$\mathbf{A}^{\boldsymbol{\mu}}_{N,\mathbf{P}_X}\mathbf{z}_N^{\boldsymbol{\mu}} = \mathbf{g}^{\boldsymbol{\mu}}_{N,\mathbf{P}_X}, \tag{31}$$

where the RB matrix $\mathbf{A}^{\boldsymbol{\mu}}_{N,\mathbf{P}_X} \in \mathbb{R}^{N\times N}$ and the RB right hand side $\mathbf{g}^{\boldsymbol{\mu}}_{N,\mathbf{P}_X} \in \mathbb{R}^N$ are defined as

$$\mathbf{A}^{\boldsymbol{\mu}}_{N,\mathbf{P}_X} = \mathbf{V}^T(\mathbf{A}_h^{\boldsymbol{\mu}})^T\mathbf{P}_X^{-1}\mathbf{A}_h^{\boldsymbol{\mu}}\mathbf{V} \qquad \mathbf{g}^{\boldsymbol{\mu}}_{N,\mathbf{P}_X} = \mathbf{V}^T(\mathbf{A}_h^{\boldsymbol{\mu}})^T\mathbf{P}_X^{-1}\mathbf{g}_h^{\boldsymbol{\mu}}. \tag{32}$$

Remark 3.2. *Equations* (32) *are similar to the ones in* (24)*, provided that* $\mathbf{X}_h^{\boldsymbol{\mu}}$ *is substituted with* $\mathbf{P}_X$*.*

In the following we provide results showing the stability of system (31) and the optimality properties satisfied by the solution $\mathbf{z}_N^{\boldsymbol{\mu}}$ of (31).

Proposition 3.2. *Assume that condition* (9) *holds,* $\mathbf{W}^{\boldsymbol{\mu}}$ *is taken as in* (30)*. and let assumption 3.1 hold. Then problem* (31) *is inf-sup stable, more precisely*

$$\beta^{\boldsymbol{\mu}}_{\mathbf{P}_X,N} = \inf_{\mathbf{z}_N\in\mathbb{R}^N}\sup_{\mathbf{w}_N\in\mathbb{R}^N}\frac{\mathbf{w}_N^T\mathbf{A}^{\boldsymbol{\mu}}_{N,\mathbf{P}_X}\mathbf{z}_N}{\|\mathbf{V}\mathbf{z}_N\|_{\mathbf{X}_h^{\boldsymbol{\mu}}}\|\mathbf{W}^{\boldsymbol{\mu}}_{\mathbf{P}_X}\mathbf{w}_N\|_{\mathbf{X}_h^{\boldsymbol{\mu}}}} \geq \frac{c}{C}\beta^{min} \qquad \forall \boldsymbol{\mu}\in\mathcal{D}. \tag{33}$$

Moreover, problem (31) *has a unique solution* $\mathbf{z}_N^{\boldsymbol{\mu}} \in \mathbb{R}^N$ *for any* $\boldsymbol{\mu}\in\mathcal{D}$*, which satisfies*

$$\|\mathbf{z}_N^{\boldsymbol{\mu}}\|_{\mathbf{X}_h^{\boldsymbol{\mu}}} \leq \frac{1}{\beta^{\boldsymbol{\mu}}_{\mathbf{P}_X,N}}\|\mathbf{g}_h^{\boldsymbol{\mu}}\|_{(\mathbf{X}_h^{\boldsymbol{\mu}})^{-1}}.$$

Proof. Starting from (29), it holds

$$\mathbf{w}_h^T\mathbf{A}_h^{\mu}\mathbf{z}_h = \mathbf{w}_h^T\mathbf{P}_X\mathbf{t}^{\mu}_{\mathbf{P}_X}(\mathbf{z}_h) \leq \|\mathbf{t}^{\mu}_{\mathbf{P}_X}(\mathbf{z}_h)\|_{\mathbf{P}_X}\|\mathbf{w}_h\|_{\mathbf{P}_X} \qquad \forall \mathbf{w}_h\in\mathbb{R}^{N_h},$$

where the equality is reached for $\mathbf{w}_h = \mathbf{t}^{\mu}_{\mathbf{P}_X}(\mathbf{z}_h)$. Consequently, using the inequalities in (26) we have

$$\begin{aligned}
\beta^{\boldsymbol{\mu}}_{\mathbf{P}_X,N} &= \inf_{\mathbf{z}_N\in\mathbb{R}^N}\sup_{\mathbf{w}_N\in\mathbb{R}^N}\frac{\mathbf{w}_N^T\mathbf{A}^{\boldsymbol{\mu}}_{N,\mathbf{P}_X}\mathbf{z}_N}{\|\mathbf{V}\mathbf{z}_N\|_{\mathbf{X}_h^{\boldsymbol{\mu}}}\|\mathbf{W}^{\boldsymbol{\mu}}_{\mathbf{P}_X}\mathbf{w}_N\|_{\mathbf{X}_h^{\boldsymbol{\mu}}}} \geq \frac{1}{C}\inf_{\mathbf{z}_N\in\mathbb{R}^N}\sup_{\mathbf{w}_N\in\mathbb{R}^N}\frac{\mathbf{w}_N^T\mathbf{A}^{\boldsymbol{\mu}}_{N,\mathbf{P}_X}\mathbf{z}_N}{\|\mathbf{V}\mathbf{z}_N\|_{\mathbf{X}_h^{\boldsymbol{\mu}}}\|\mathbf{W}^{\boldsymbol{\mu}}_{\mathbf{P}_X}\mathbf{w}_N\|_{\mathbf{P}_X}}\\
&= \frac{1}{C}\inf_{\mathbf{z}_N\in\mathbb{R}^N}\frac{\|\mathbf{t}^{\mu}_{\mathbf{P}_X}(\mathbf{V}\mathbf{z}_N)\|_{\mathbf{P}_X}}{\|\mathbf{V}\mathbf{z}_N\|_{\mathbf{X}_h^{\mu}}} \geq \frac{1}{C}\inf_{\mathbf{z}_h\in\mathbb{R}^{N_h}}\frac{\|\mathbf{t}^{\mu}_{\mathbf{P}_X}(\mathbf{z}_h)\|_{\mathbf{P}_X}}{\|\mathbf{z}_h\|_{\mathbf{X}_h^{\mu}}}\\
&= \frac{1}{C}\inf_{\mathbf{z}_h\in\mathbb{R}^{N_h}}\sup_{\mathbf{w}_h\in\mathbb{R}^{N_h}}\frac{\mathbf{w}_h^T\mathbf{A}_h^{\boldsymbol{\mu}}\mathbf{z}_h}{\|\mathbf{z}_h\|_{\mathbf{X}_h^{\boldsymbol{\mu}}}\|\mathbf{w}_h\|_{\mathbf{P}_X}} \geq \frac{c}{C}\inf_{\mathbf{z}_h\in\mathbb{R}^{N_h}}\sup_{\mathbf{w}_h\in\mathbb{R}^{N_h}}\frac{\mathbf{w}_h^T\mathbf{A}_h^{\boldsymbol{\mu}}\mathbf{z}_h}{\|\mathbf{z}_h\|_{\mathbf{X}_h^{\boldsymbol{\mu}}}\|\mathbf{w}_h\|_{\mathbf{X}_h^{\boldsymbol{\mu}}}}\\
&= \frac{c}{C}\beta_h^{\boldsymbol{\mu}} \geq \frac{c}{C}\beta^{min}.
\end{aligned}$$

By applying the Babuška theorem for non-coercive problems satisfying an *inf-sup* stability property, see [2], concludes the proof. ☐

Proposition 3.3. *Let assumption 3.1 hold, then problem* (31) *corresponds to solving the minimization problem*

$$\mathbf{z}_N^{\boldsymbol{\mu}} = \arg\min_{\mathbf{v}_N\in\mathbb{R}^N}\|\mathbf{g}_h^{\boldsymbol{\mu}} - \mathbf{A}_h^{\boldsymbol{\mu}}\mathbf{V}\mathbf{v}_N\|^2_{\mathbf{P}_X^{-1}}. \tag{34}$$

Proof. We consider the quadratic functional

$$J(\mathbf{v}_N) = \|\mathbf{g}_h^{\boldsymbol{\mu}} - \mathbf{A}_h^{\boldsymbol{\mu}}\mathbf{V}\mathbf{v}_N\|^2_{\mathbf{P}_X^{-1}}, \quad \mathbf{v}_N\in\mathbb{R}^N,$$

which has a unique minimum in $\mathbf{u}_N \in \mathbb{R}^N$ thanks to the nonsingularity of the matrices $\mathbf{P}_X$ and $\mathbf{A}_h^{\boldsymbol{\mu}}$. We impose its gradient with respect to $\mathbf{v}_N$ and evaluated at $\mathbf{u}_N$ to vanish. By employing the definition of the norm $\|\cdot\|_{\mathbf{P}_X^{-1}}$ we obtain

$$
\begin{aligned}
\mathbf{0} &= \frac{\partial J\{\mathbf{v}_N\}}{\partial \mathbf{v}_N}(\mathbf{u}_N) \\
&= \frac{\partial}{\partial \mathbf{v}_N}\Big\{(\mathbf{g}_h^{\boldsymbol{\mu}})^T\mathbf{P}_X^{-1}\mathbf{g}_h^{\boldsymbol{\mu}} + \mathbf{v}_N^T\mathbf{V}^T(\mathbf{A}_h^{\boldsymbol{\mu}})^T\mathbf{P}_X^{-1}\mathbf{A}_h^{\boldsymbol{\mu}}\mathbf{V}\mathbf{v}_N - 2(\mathbf{g}_h^{\boldsymbol{\mu}})^T\mathbf{P}_X^{-1}\mathbf{A}_h^{\boldsymbol{\mu}}\mathbf{V}\mathbf{v}_N\Big\}(\mathbf{u}_N) \\
&= 2\mathbf{V}^T(\mathbf{A}_h^{\boldsymbol{\mu}})^T\mathbf{P}_X^{-1}\mathbf{A}_h^{\boldsymbol{\mu}}\mathbf{V}\mathbf{u}_N - 2(\mathbf{g}_h^{\boldsymbol{\mu}})^T\mathbf{P}_X^{-1}\mathbf{A}_h^{\boldsymbol{\mu}}\mathbf{V}\mathbf{u}_N = 2\mathbf{A}_{N,\mathbf{P}_X}^{\boldsymbol{\mu}}\mathbf{u}_N - 2\mathbf{g}_{N,\mathbf{P}_X}^{\boldsymbol{\mu}}.
\end{aligned}
$$

Therefore, $\mathbf{u}_N$ is such that

$$
\mathbf{A}_{N,\mathbf{P}_X}^{\boldsymbol{\mu}}\mathbf{u}_N = \mathbf{g}_{N,\mathbf{P}_X}^{\boldsymbol{\mu}},
$$

hence it coincides with the RB solution $\mathbf{z}_N^{\boldsymbol{\mu}}$, since the matrix $\mathbf{A}_{N,\mathbf{P}_X}^{\boldsymbol{\mu}}$ is invertible. □

3.3.1 Assembling the RB problem

When building a RB approximation, it is essential to assume the affine dependence on $\boldsymbol{\mu}$ in the FE arrays (7), that is

$$
\mathbf{A}_h^{\boldsymbol{\mu}} = \sum_{q=1}^{Q_a}\Theta_a^q(\boldsymbol{\mu})\mathbf{A}_h^q, \qquad \mathbf{g}_h^{\boldsymbol{\mu}} = \sum_{q=1}^{Q_g}\Theta_g^q(\boldsymbol{\mu})\mathbf{g}_h^q, \tag{35}
$$

where $\Theta_a^q : \mathcal{D} \to \mathbb{R}$, $q = 1,\dots,Q_a$ and $\Theta_g^q : \mathcal{D} \to \mathbb{R}$, $q = 1,\dots,Q_g$ are $\boldsymbol{\mu}$-dependent functions, while the matrices $\mathbf{A}_h^q \in \mathbb{R}^{N_h\times N_h}$ and the vectors $\mathbf{g}_h^q \in \mathbb{R}^{N_h}$ are $\boldsymbol{\mu}$-independent. If assumption (35) is verified, then the RB algebraic structures can be written, for the aLS-RB case, as

$$
\begin{aligned}
\mathbf{A}_{N,\mathbf{P}_X}^{\boldsymbol{\mu}} &= \sum_{q_1,q_2=1}^{Q_a}\Theta_a^{q_1}(\boldsymbol{\mu})\Theta_a^{q_2}(\boldsymbol{\mu})\mathbf{V}^T(\mathbf{A}_h^{q_1})^T\mathbf{P}_X^{-1}\mathbf{A}_h^{q_2}\mathbf{V} \\
&= \sum_{q_1,q_2=1}^{Q_a}\Theta_a^{q_1}(\boldsymbol{\mu})\Theta_a^{q_2}(\boldsymbol{\mu})\mathbf{A}_N^{q_1,q_2}
\end{aligned} \tag{36}
$$

$$
\begin{aligned}
\mathbf{g}_{N,\mathbf{P}_X}^{\boldsymbol{\mu}} &= \sum_{q_1=1}^{Q_a}\sum_{q_2=1}^{Q_g}\Theta_a^{q_1}(\boldsymbol{\mu})\Theta_g^{q}(\boldsymbol{\mu})\mathbf{V}^T(\mathbf{A}_h^{q_1})^T\mathbf{P}_X^{-1}\mathbf{g}_h^{q_2} \\
&= \sum_{q_1=1}^{Q_a}\sum_{q_2=1}^{Q_g}\Theta_a^{q_1}(\boldsymbol{\mu})\Theta_g^{q_2}(\boldsymbol{\mu})\mathbf{g}_N^{q_1,q_2}.
\end{aligned} \tag{37}
$$

In the G-RB case, the algebraic RB structures can be instead obtained as

$$
\mathbf{A}_N^{\boldsymbol{\mu}} = \sum_{q=1}^{Q_a}\Theta_a^q(\boldsymbol{\mu})\mathbf{V}^T\mathbf{A}_h^q\mathbf{V} = \sum_{q=1}^{Q_a}\Theta_a^q(\boldsymbol{\mu})\mathbf{A}_N^q \tag{38}
$$

$$
\mathbf{g}_N^{\boldsymbol{\mu}} = \sum_{q=1}^{Q_g}\Theta_g^q(\boldsymbol{\mu})\mathbf{V}^T\mathbf{g}_h^q = \sum_{q=1}^{Q_g}\Theta_g^q(\boldsymbol{\mu})\mathbf{g}_N^q. \tag{39}
$$

The matrices $\mathbf{A}_N^q$, $q = 1,\dots,Q_a$, $\mathbf{A}_N^{q_1,q_2} \in \mathbb{R}^{N\times N}$, $q_1, q_2 = 1,\dots,Q_a$, and the vectors $\mathbf{g}_N^q \in \mathbb{R}^N$, $q = 1,\dots,Q_g$, $\mathbf{g}_N^{q_1,q_2} \in \mathbb{R}^N$, $q_1 = 1,\dots,Q_a$, $q_2 = 1,\dots,Q_g$ can be precomputed and stored during the offline phase. During the online phase, only the sums in (36)–(37) and (38)–(39) must be calculated out to assemble the RB problem. Notice that the construction of $\mathbf{A}_N^{\boldsymbol{\mu}}$ and $\mathbf{g}_N^{\boldsymbol{\mu}}$ in (38)–(39) depends linearly on the number of affine terms Q_a and Q_g for the G-RB method. On the other hand, the corresponding aLS-RB structures $\mathbf{A}_{N,\mathbf{P}_X}^{\boldsymbol{\mu}}$ and $\mathbf{g}_{N,\mathbf{P}_X}^{\boldsymbol{\mu}}$ in (36)–(37) depend quadratically Q_a and Q_g. Practically, by employing the G-RB method softens the dependence on the number of affine terms, since less RB structures must be assembled and stored with respect to the aLS-RB method. This advantage is also visible in the online phase, since the construction of the RB matrix and right hand side scale linearly with respect to Q_a and Q_g. However, the aLS-RB matrices and right hand sides have a smaller dimension, since the velocity basis is not augmented, entailing a lower cost for computing and storing each array and for computing the solution of the RB system. Finally, notice that the affine decomposition (35) would not be exploitable in the case of standard LS-RB method, due to the $\boldsymbol{\mu}-$dependence of the matrix $\mathbf{X}_h^{\boldsymbol{\mu}}$. Indeed, one would need also an affine decomposition of $(\mathbf{X}_h^{\boldsymbol{\mu}})^{-1}$, which is generally not available since it is never explicitly assembled and its application is performed by solving a linear system where $\mathbf{X}_h^{\boldsymbol{\mu}}$ is at the left hand side.

In the numerical examples considered in this work, as well as in almost every problem of applied interest, the geometrical dependence of the computational domain on the parameter $\boldsymbol{\mu}$ is generally nonaffine, therefore an affine representation of $\mathbf{A}_h^{\boldsymbol{\mu}}$ and $\mathbf{g}_h^{\boldsymbol{\mu}}$ cannot be computed. To circumvent this problem both the empirical interpolation method (EIM) or its discrete variants DEIM and Matrix-DEIM [5, 15, 30] offer the possibility to recover an *approximate* affine decomposition. When such techniques are employed, the relations (35) are satisfied up to a certain tolerance,

$$\mathbf{A}_h^{\boldsymbol{\mu}} \approx \sum_{q=1}^{Q_a} \tilde{\Theta}_a^q(\boldsymbol{\mu})\mathbf{A}_h^q, \qquad \mathbf{g}_h^{\boldsymbol{\mu}} \approx \sum_{q=1}^{Q_g} \tilde{\Theta}_g^q(\boldsymbol{\mu})\mathbf{g}_h^q. \tag{40}$$

Q_a and Q_g are the number of selected basis computed by the corresponding algorithms. In the case of DEIM (resp. M-DEIM), the basis are again built through POD on a set of n_s vectors (resp. matrices) snapshots and up to a provided tolerance δ_{deim}. Then, for a new value of the parameter $\boldsymbol{\mu}$, the coefficients $\tilde{\Theta}_g^q : \mathcal{D} \to \mathbb{R}\, q = 1, \dots, Q_a$ (resp. $\tilde{\Theta}_a^q : \mathcal{D} \to \mathbb{R}$, $q = 1, \dots, Q_g$) are computed by solving an interpolation problem.

3.3.2 On the choice of $\mathbf{P}_X$

A natural question arising in this context regards the choice of the matrix $\mathbf{P}_X$, since this directly affects the values of the constants c and C; from (33). These constants play indeed a relevant role in the ill-conditioning of the aLS-RB approximation. Moreover, it is clear that by taking $\mathbf{P}_X = \mathbf{X}_h^{\boldsymbol{\mu}}$ we would have the optimal case $c/C = 1$, hence recovering the standard LS-RB method. Therefore, $\mathbf{P}_X$ should be chosen as close as possible to $\mathbf{X}_h^{\boldsymbol{\mu}}$, however it has to be $\boldsymbol{\mu}$-independent. The following results give some insights on how to properly choose the matrix $\mathbf{P}_X$. Their proofs are reported in the appendix A.

Lemma 3.2. *Let assumption 3.1 hold. The optimal value for the constants $C \geq c$ satisfying* (26) *are*

$$C = \|\mathbf{P}_X^{-1/2}(\mathbf{X}_h^{\boldsymbol{\mu}})^{1/2}\|_{\mathbf{P}_X}, \qquad c = 1/\|(\mathbf{X}_h^{\boldsymbol{\mu}})^{-1/2}\mathbf{P}_X^{1/2}\|_{\mathbf{X}_h^{\boldsymbol{\mu}}}. \tag{41}$$

From now, we consider C, c as their optimal values (41).

Lemma 3.3. *Let assumption 3.1 hold. The two constants $C \geq c > 0$ satisfying* (26) *and* (41) *are such that*

$$\frac{c}{C} = \left[\mathcal{K}_{\mathbf{X}_h}(\mathbf{P}_X^{-1}\mathbf{X}_h^{\boldsymbol{\mu}})\right]^{-1/2} = \left[\mathcal{K}_2(\mathbf{P}_X^{-1/2}\mathbf{X}_h\mathbf{P}_X^{-1/2})\right]^{-1/2}. \tag{42}$$

It is clear from Lemma 3.3 that the matrix $\mathbf{P}_X$ should be chosen in such a way that the condition number of the preconditioned matrix $\mathbf{P}_X^{-1}\mathbf{X}_h^{\boldsymbol{\mu}}$ does not depend on the mesh size h, i.e. $\mathbf{P}_X$ should be an optimal preconditioner for $\mathbf{X}_h^{\boldsymbol{\mu}}$. If this is not the case, the value of the stability constant of the RB approximation $\beta^{\boldsymbol{\mu}}_{\mathbf{P}_X,N}$ may depend on h. Furthermore, if we set up our RB approximation in a HPC environment, employing a mesh partitioner to divide the computational domain among the processors, it is also advisable to choose $\mathbf{P}_X$ such that $\frac{c}{C}$ does not depend on the size H of the subdomains, i.e. $\mathbf{P}_X$ should be a scalable preconditioner for $\mathbf{X}_h^{\boldsymbol{\mu}}$.

In our numerical experiments $\mathbf{P}_X$ is chosen either as $\mathbf{P}_X = \mathbf{X}_h^0$, i.e. as the norm matrix in the reference domain, or as a block diagonal preconditioner of $\mathbf{X}_h^0$, where the two blocks are generated as symmetric and positive definite preconditioners $\mathbf{P}_{\mathbf{X}_u} \in \mathbb{R}^{N_h^u \times N_h^u}$ of $\mathbf{X}_u^0$ and $\mathbf{P}_{\mathbf{X}_p} \in \mathbb{R}^{N_h^p \times N_h^p}$ of $\mathbf{X}_p^0$.

4 Numerical experiments

We show the results obtained with the RB methods presented in Section 3 implemented within the LifeV [9] library. We compare the G-RB method (with velocity enrichment) and the aLS-RB method in the case of large-scale Stokes flows in a cylindrical domain which is nonaffinely parametrized. The deformation is not analitically known, since it is retrieved as the solution of an additional FE problem which harmonically extends in the interior of the domain the datum prescribed on a Dirichlet boundary. In the following sections, we present the setup of the problem.

4.1 Test case setting: Stokes problem in a parametrized cylinder

We consider the Stokes equations in a parameter dependent domain $\Omega^{\boldsymbol{\mu}} \subset \mathbb{R}^3$, which is obtained by deforming a reference domain

$$\Omega^0 = \{\vec{x} \in \mathbb{R}^3 : \ x_1^2 + x_1^2 < 0.25, \, x_3 \in (0, 5)\}$$

by means of a displacement $\vec{d}^{\boldsymbol{\mu}}$ obtained as the harmonic extension of a boundary deformation. More specifically, we set

$$\Omega^{\boldsymbol{\mu}} = \{\vec{x}^{\boldsymbol{\mu}} \in \mathbb{R}^3 : \ \vec{x}^{\boldsymbol{\mu}} = \vec{x} + \vec{d}^{\boldsymbol{\mu}}\},$$

where $\vec{d}^{\boldsymbol{\mu}}$ solves the following PDE

$$\begin{cases} -\Delta \vec{d}^{\boldsymbol{\mu}} = \vec{0} & \text{in } \Omega^0 \\ \vec{d}^{\boldsymbol{\mu}} = \vec{h}^{\boldsymbol{\mu}} & \text{on } \partial\Omega^0. \end{cases} \tag{43}$$

In our numerical experiments we take $\boldsymbol{\mu} = (\mu_1, \mu_2) \in \mathcal{D} = [-0.3, \, 0.3] \times [2, \, 3]$ and a Dirichlet datum of the form

$$\vec{h}^{\boldsymbol{\mu}} = \begin{bmatrix} -x_1 \mu_1 \exp\{-5(x_3 - \mu_2)^2\} \\ -x_2 \mu_1 \exp\{-5(x_3 - \mu_2)^2\} \\ 0 \end{bmatrix},$$

entailing a deformation of the cylinder by narrowing or enlarging (according to the sign of μ_2) its section in different positions along the coordinate x_3 (according to the value of μ_1). Notice that the solution $\vec{d}^{\boldsymbol{\mu}}$ of (43) is not known a-priori, therefore we compute its numerical approximation $\vec{d}_h^{\boldsymbol{\mu}}$ by writing the variational form of problem (43) and by employing the FE method. We denote by $\mathbf{d}_h^{\boldsymbol{\mu}} \in \mathbb{R}^{N_h^d}$ the solution of the corresponding FE linear system.

Moreover, once the computational domain has been deformed, the lifting function $\vec{r}_{\vec{g}_D}^{\boldsymbol{\mu}}$ is computed similarly by solving the following problem

$$\begin{cases} -\Delta \vec{r}_{\vec{g}_D}^{\boldsymbol{\mu}} = \vec{0} & \text{in } \Omega^{\boldsymbol{\mu}} \\ \vec{r}_{\vec{g}_D}^{\boldsymbol{\mu}} = \vec{g}_D^{\boldsymbol{\mu}} & \text{on } \Gamma_{in}^{\boldsymbol{\mu}} \\ \vec{r}_{\vec{g}_D}^{\boldsymbol{\mu}} = \vec{0} & \text{on } \Gamma_w^{\boldsymbol{\mu}} \\ \frac{\partial \vec{r}_{\vec{g}_D}^{\boldsymbol{\mu}}}{\partial \vec{n}^{\boldsymbol{\mu}}} = \vec{0} & \text{on } \Gamma_{out}^{\boldsymbol{\mu}}, \end{cases} \tag{44}$$

which is an harmonic extension of the Dirichlet data in (2). Here $\vec{g}_D^{\boldsymbol{\mu}}$ is a parabolic profile such that the flow rate at the inlet is equal to 1. Problem (44) as well is discretized with the FE method with second order polynomials ($\mathbb{P}^2$) basis functions, leading to a parametrized linear system whose solution $\mathbf{r}_h^{\boldsymbol{\mu}} \in \mathbb{R}^{N_h^u}$ is the approximated lifting functions. In Fig. 1, the deformation $\mathbf{d}_h^{\boldsymbol{\mu}}$ is reported for three different values of $\boldsymbol{\mu} \in \mathcal{D}$. In the numerical experiments we present, Taylor-Hood FE ($\mathbb{P}^2 - \mathbb{P}^1$), with a mesh leading to

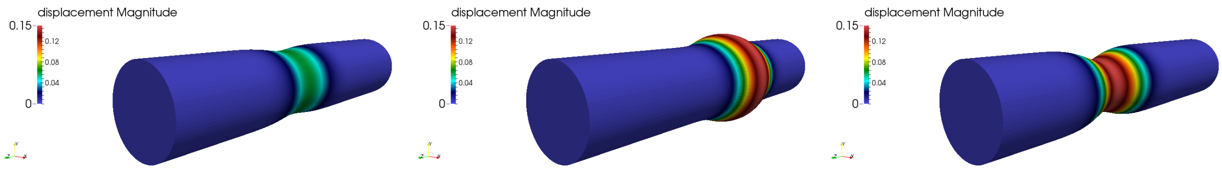

(a) $\boldsymbol{\mu} = (2.7, 0.12)$ (b) $\boldsymbol{\mu} = (2, -0.3)$ (c) $\boldsymbol{\mu} = (3, 0.3)$

Figure 1: Displacement for different values of $\boldsymbol{\mu}$.

$N_h = N_h^u + N_h^p = 1'503'280 + 64'943 = 1'568'223$ degrees of freedom, are employed for the Stokes equations. The algebraic problem is run on the Piz-Daint cluster with Cray XC40 machines, at the Swiss National Supercomputing Center (CSCS) in Lugano. The computation has been carried out with 256 processors.

4.1.1 FE simulation setup

For any parameter $\boldsymbol{\mu}$ considered, we solve the FE problems to approximate the deformation $\vec{d}^{\boldsymbol{\mu}}$ of problem (43) and the lifting function $\vec{r}^{\boldsymbol{\mu}}_{\vec{g}_D}$ of problem (44). The associated algebraic systems are solved by the preconditioned CG method, with a tolerance on the Euclidean norm of the residual (rescaled with the Euclidean norm of the right hand side) of 10^{-8}. An algebraic multigrid (AMG) preconditioner from the ML package of Trilinos, see [22], is employed. Once computed the deformation for a new parameter value $\boldsymbol{\mu}$, we employ a move-mesh tool to shape the computational domain and assemble the FE arrays. This ensures that the meshes for different instances of the parameter $\boldsymbol{\mu}$ are topologically equivalent and there is a one-to-one correspondence between degrees of freedom.

The linear system (7) resulting from the FE discretization of the Stokes equations is solved with the preconditioned flexible GMRES (FGMRES) method, where the preconditioner is the Pressure Mass Matrix (PMM) operator, which exploits the block structure of (8) and employs the mass matrix in pressure to approximate the Schur complement, see [32]. It entails at every iteration the solution of a problem for the velocity (involving the velocity stiffness matrix) and one for the pressure (involving the pressure mass matrix). Both linear systems are solved inexactly with the preconditioned CG method, where the preconditioner is still the AMG preconditioner from the ML package of Trilinos, this time with a tolerance on the euclidean norm of the residual (rescaled with the euclidean norm of the right hand side) of 10^{-5}. Notice that we employed the FGMRES (instead of regular GMRES) due to the use of inner iterations for the problems involving the velocity and the pressure, which, as a matter of fact, yield an iteration dependent preconditioner. The PMM preconditioner provides satisfactory results in the case of the Stokes equations, cf. [36, 21]. Finally, in order to compute the FE solution with the flexible GMRES method, up to a final tolerance of 10^{-8}, our solver requires on average of 38.0 seconds, which also accounts for the time for deforming the domain, building the lifting function, the PMM preconditioner and the FE solution. In particular, computing the deformation $\mathbf{d}_h^{\boldsymbol{\mu}}$ and the lifting function $\mathbf{r}_h^{\boldsymbol{\mu}}$ requires 2.5 seconds (6.5% of the FE simulation).

4.1.2 RB simulation setup

During the *offline* phase, we explore the parameter domain $\mathcal{D}$ for building our RB approximation. In particular we perform the following steps:

- we randomly choose a set of $n_s = 150$ parameters $\{\boldsymbol{\mu}_i\}_{i=1}^{n_s} \subset \mathcal{D}$; then we compute the corresponding velocity snapshots $\{\mathbf{u}_h^{\boldsymbol{\mu}_i}\}_{i=1}^{n_s}$ and pressure snapshots $\{\mathbf{p}_h^{\boldsymbol{\mu}_i}\}_{i=1}^{n_s}$ by solving the corresponding linear system (7). Next, we build the RB space V_N by separately computing a basis $\mathbf{V}^u_{N_u}$ for the velocity and $\mathbf{V}^p_{N_p}$ the pressure, by plugging in the POD the same tolerance $\varepsilon_{\text{POD}} = \delta_{RB}$ in both cases. If the Galerkin-RB method with velocity enrichment is employed, we also compute $n_s = 150$ supremizer snapshots $\{\mathbf{t}_p^{\boldsymbol{\mu}_i}(\mathbf{p}_h^{\boldsymbol{\mu}_i})\}_{i=1}^{n_s}$. Since in general we do not take the same number of basis functions for the velocity and pressure RB spaces, we use a tolerance also for computing the pressure supremizer basis functions. With this aim, we employ POD with $\varepsilon_{\text{POD}} = \frac{\delta_{RB}}{10}$ to build the supremizer basis $\mathbf{V}^s_{N_s}$, which numerically confirmed to provide a stable G-RB problem.
- we compute a basis to affinely approximate $\mathbf{f}_h^{\boldsymbol{\mu}}$, $\mathbf{r}_h^{\boldsymbol{\mu}}$ (with DEIM) and $\mathbf{D}_h^{\boldsymbol{\mu}}$, $\mathbf{B}_h^{\boldsymbol{\mu}}$ (with M-DEIM), by taking $n_s = 100$ snapshots for each of these quantities and a tolerance δ_{deim} to be plugged in the POD.

In the *online* phase, we perform an analysis of the G-RB and aLS-RB methods with respect to the tolerances δ_{RB} (or the number of basis functions N) and δ_{deim}, by choosing δ_{RB}, $\delta_{\text{deim}} = 10^{-l}$, $l = 2, 3, 4, 5, 6$. We evaluate the accuracy of the RB solutions $\mathbf{z}_N^{\boldsymbol{\mu}}$ in terms of the rescaled RB residual

$$r_{RB} = \frac{\|\mathbf{g}_h^{\boldsymbol{\mu}} - \mathbf{A}_h^{\boldsymbol{\mu}} \mathbf{V} \mathbf{z}_N^{\boldsymbol{\mu}}\|_{(\mathbf{X}_h^{\boldsymbol{\mu}})^{-1}}}{\|\mathbf{g}_h^{\boldsymbol{\mu}}\|_{(\mathbf{X}_h^{\boldsymbol{\mu}})^{-1}}},$$

averaging the results obtained for $N_{onl} = 100$ parameters, different from the one employed within the offline phase. For the aLS-RB method, we present the results for two choices of the matrix $\mathbf{P}_X$:

- $\mathbf{P}_X = \mathbf{X}_h^0$, i.e. we approximate $\mathbf{X}_h^{\boldsymbol{\mu}}$ with the matrix norm on the reference domain Ω^0. With this aim, in the offline phase, we need to solve FE linear systems with $\mathbf{X}_h^0$ on the left hand side to compute the affine terms $\mathbf{A}_N^{q_1,q_2}$, $q_1, q_2 = 1, \ldots, Q_a$. These linear systems are solved with the CG method preconditioned with AMG, up to a tolerance of 10^{-8} on the euclidean norm of the relative residual;
- $\mathbf{P}_X = \mathbf{P}_{\mathbf{X}_h^0}$, i.e. we take the preconditioner $\mathbf{P}_{\mathbf{X}_u^0}$ of $\mathbf{X}_h^{\boldsymbol{\mu}}$, which has a block structure $\mathbf{P}_{\mathbf{X}_h^0} = diag(\mathbf{P}_{\mathbf{X}_u^0}, \mathbf{P}_{\mathbf{X}_p^0})$, where $\mathbf{P}_{\mathbf{X}_u} \in \mathbb{R}^{N_h^u \times N_h^u}$ (resp. $\mathbf{P}_{\mathbf{X}_p} \in \mathbb{R}^{N_h^p \times N_h^p}$) is a symmetric and positive definite AMG preconditioner of $\mathbf{X}_u^0$ (resp. $\mathbf{X}_p^0$).

Both choices lead to a matrix $\mathbf{P}_X$ which does not depend on $\boldsymbol{\mu}$. Notice that for any new parameter $\boldsymbol{\mu}$ considered online, we solve the FE linear system for computing the deformation $\mathbf{d}_h^{\boldsymbol{\mu}}$ and the lifting function $\mathbf{r}_h^{\boldsymbol{\mu}}$. Alternatively, we could compute through the RB method the RB approximations of $\mathbf{d}_h^{\boldsymbol{\mu}}$ and $\mathbf{r}_h^{\boldsymbol{\mu}}$, to be exploited during the online phase, similarly to what has been proposed in [27] for the parametrized Helmholtz scattering problem. However this goes beyond the scope of this paper and will be the subject of further research.

4.2 Numerical results

4.2.1 Offline phase

In Tables 1-2 we show the offline time required to build the structures of the RB approximations when using $\delta_{RB} = \delta_{\text{deim}} = 10^{-6}$ (comparable results hold when bigger tolerances are used). We recall that δ_{RB} is used within POD to build the velocity and pressure RB spaces, while δ_{deim} for building an affine approximation of the FE blocks of $\mathbf{A}_h^{\boldsymbol{\mu}}$ and $\mathbf{g}_h$ in the (M-)DEIM algorithm. In the first table, we report the computational times to build the (M-)DEIM basis which provide an affine approximation of the FE matrices and right hand sides; these times are shared by both the G-RB and aLSRB methods. In the second table, the total time of the offline computation is reported, together with the details of its three main stages: snapshots computation, POD and RB affine arrays construction. Snapshots computation is the most demanding phase, and is particularly expensive if the G-RB method is employed, since it entails the additional computation of n_s pressure supremizer snapshots $\left\{\mathbf{t}_p^{\boldsymbol{\mu}_i}(\mathbf{p}_h^{\boldsymbol{\mu}_i})\right\}_{i=1}^{n_s}$. The second phase, involving the POD to build the RB spaces, only requires a tiny percentage of the offline time for all the three methods considered, however also in this case, the two variants of the aLS-RB method need a shorter time than the G-RB method, because they require only the construction of the velocity and pressure spaces $\mathbf{V}_{N_u}^u$ and $\mathbf{V}_{N_p}^p$, while in the G-RB case the pressure supremizer space $\mathbf{V}_{N_s}^s$ must also be constructed. Concerning the construction of the affine RB matrices and vectors, the G-RB method scales linearly on the number (Q_a and Q_g) of affine terms of the FE matrices and right hand sides, yielding a computational time which is shorter than the one obtained with the aLS-RB methods for this phase. However, there is also a significant difference between the two variants of aLS-RB method. By employing $\mathbf{P}_X = \mathbf{X}_h^0$, for assembling the affine terms $\mathbf{A}_N^{q_1,q_2}$, $q_1, q_2 = 1, \ldots, Q_a$, a FE linear system must be solved for each combination of the N RB functions $\{\boldsymbol{\xi}_i\}_{i=1}^N$ and Q_a affine terms $\{\mathbf{A}_h^q\}_{q=1}^{Q_a}$, leading to $N \cdot Q_a$ FE linear systems. On the other hand, by employing $\mathbf{P}_X = \mathbf{P}_{\mathbf{X}_h^0}$, only $N \cdot Q_a$ applications of $\mathbf{P}_{\mathbf{X}_h^0}^{-1}$ need to be performed, boosting the computation of the affine RB structures. Finally, the lowest offline time is required by the aLS-RB method where $\mathbf{P}_X = \mathbf{P}_{\mathbf{X}_h^0}$ is employed, performing the offline phase in about 81% of the time required by the aLS-RB method with $\mathbf{P}_X = \mathbf{X}_h^0$ and 96% of the time required by the G-RB method. This is due to the fact it simultaneously does not require the construction of the pressure supremizing snapshots to augment the velocity RB space and to cheaply construct the RB affine arrays.

In Figure 2 the number of RB functions (left) and (M-)DEIM affine terms are reported as function of the tolerances δ_{RB} and δ_{deim}, respectively. The number of pressure RB functions is the same for the G-RB and aLS-RB method, however the number of velocity basis functions doubles in the former case, due to the velocity enrichment required to ensure the well-posedness of the resulting G-RB approximation.

Table 1: Computational time (seconds) to build RB basis with $\delta_{RB} = 10^{-6}$.

MDEIM - $\mathbf{D}_h^{\boldsymbol{\mu}}$	MDEIM - $\mathbf{B}_h^{\boldsymbol{\mu}}$	DEIM - $\mathbf{f}_h^{\boldsymbol{\mu}}$	DEIM - $\mathbf{r}_h^{\boldsymbol{\mu}}$	Total (M-)DEIM
362.6	249.4	326.7	321.3	1260.0

Table 2: Computational time (seconds) to build (M-)DEIM affine basis with $\delta_{\text{deim}} = 10^{-6}$.

	G-RB	aLS-RB ($\mathbf{X}_h^0$)	aLS-RB ($\mathbf{P}_{\mathbf{X}_h^0}$)
Snapshots computation	6102.2	5699.4	5699.4
POD	3.5	2.1	2.1
Affine arrays construction	19.6	1789.8	153.3
Total (M-)DEIM	1260.0	1260.0	1260.0
Total offline phase	7385.3	8751.3	7114.8

4.2.2 Online phase

In Fig. 3, 4 and 5 the FE solution computed for different values of the parameter and the corresponding errors obtained with the G-RB method and the aLS-RB method with $\mathbf{P}_X = \mathbf{X}_h^0$ are shown (the aLS-RB

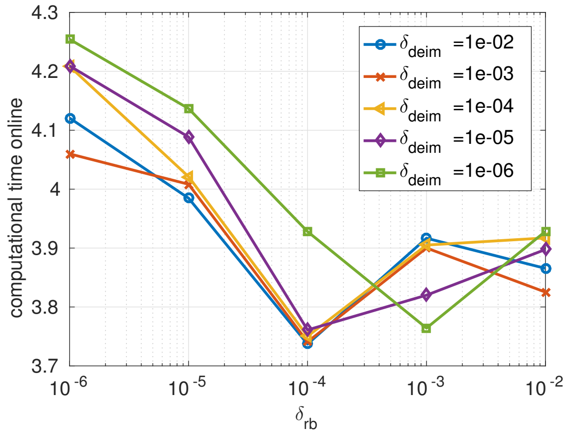

(a) RB.

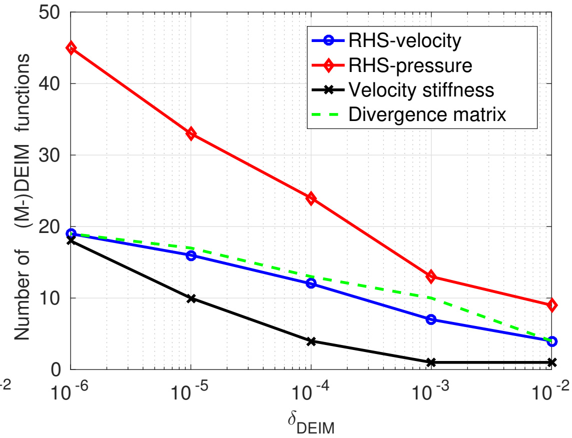

(b) (M-)DEIM.

Figure 2: RB and (M-)DEIM functions vs δ_{RB}, $\delta_{\text{deim}} = 10^{-l}$, $l = 2, 3, 4, 5, 6$.

method with $\mathbf{P}_X = \mathbf{P}_{\mathbf{X}_h^0}$ provides similar results).

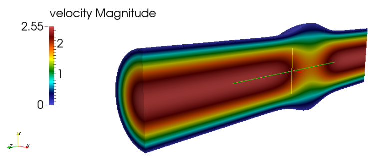

(a) FE velocity magnitude.

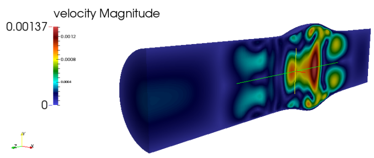

(b) G-RB velocity error magnitude.

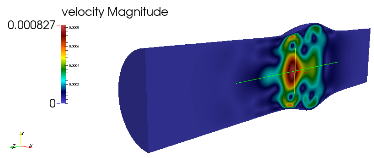

(c) aLS-RB velocity error magnitude.

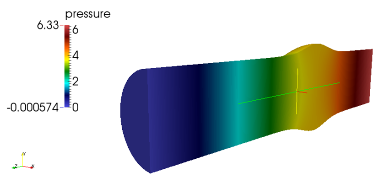

(d) FE pressure

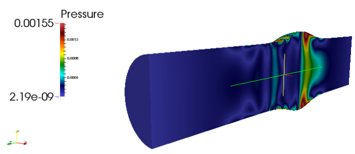

(e) G-RB norm of pressure error.

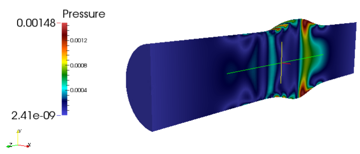

(f) aLS-RB norm of pressure error.

Figure 3: FE solution and G-RB and aLS-RB errors for $\boldsymbol{\mu} = (2, -0.3)$.

The proposed aLS-RB method, either with $\mathbf{P}_X = \mathbf{X}_h^0$ or $\mathbf{P}_X = \mathbf{P}_{\mathbf{X}_h^0}$, allows to obtain an exponential decay of the residual r_{RB} with respect to the number of RB functions N; the trend, in loglog scale, is reported in Fig. 6. A tolerance $\delta_{\text{deim}} = 10^{-8}$ has been used for (M-)DEIM algorithms, in order to consider negligible the error induced by affinely approximating the FE arrays.

An analysis of the convergence of the residual r_{RB} with varying both the tolerances δ_{RB}, $\delta_{\text{deim}} = 10^{-l}$, $l = 2, 3, 4, 5, 6$ is reported in Fig. 7 for the G-RB and the two variants of the aLS-RB methods. By using the same tolerances δ_{deim} and δ_{RB}, the aLS-RB method allows to compute a more accurate solution during the online phase of about 1 order of magnitude. Moreover, notice that by using the same δ_{deim} for the aLS-RB methods and the G-RB method, the latter requires a lower tolerance δ_{RB} to reach a solution with the same accuracy, yielding a much larger number of RB functions N. Obtaining a more accurate solution with the aLS-RB method is an expected result, since the standard LS-RB method seeks a RB approximation minimizing the $(\mathbf{X}_h^{\boldsymbol{\mu}})^{-1}$ norm of the residual, and the aLS-RB method provides a RB approximation minimizing the $\mathbf{P}_X^{-1}$ norm, where $\mathbf{P}_X^{-1} \approx (\mathbf{X}_h^{\boldsymbol{\mu}})^{-1}$, as shown in Proposition 3.3.

In Fig. 7, the computational time required to assemble and solve the RB problem is reported for the three methods by varying both the tolerances δ_{RB}, $\delta_{\text{deim}} = 10^{-l}$, $l = 2, 3, 4, 5, 6$. Depending on the desired level of accuracy and the RB method employed, the computational time required to solve the RB problem online ranges from 3.75 to 4.3 seconds. Therefore, a solution accurate up to an error of 0.01% on the FE residual r_{RB} is computed in a time ranging from 10% to 12% of the time required by the FE simulation.

Notice however that the online computational time accounts also for the time employed for assembling

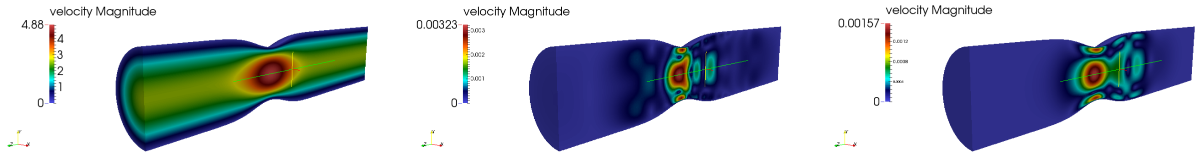

(a) FE velocity magnitude. (b) G-RB velocity error magnitude. (c) aLS-RB velocity error magnitude.

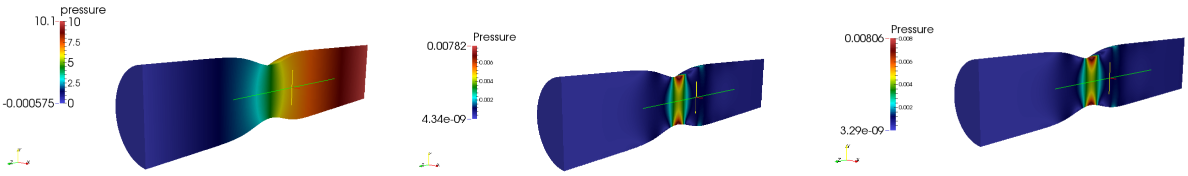

(d) FE pressure (e) G-RB norm of pressure error. (f) aLS-RB norm of pressure error.

Figure 4: FE solution and G-RB and aLS-RB errors for $\boldsymbol{\mu} = (3, 0.3)$.

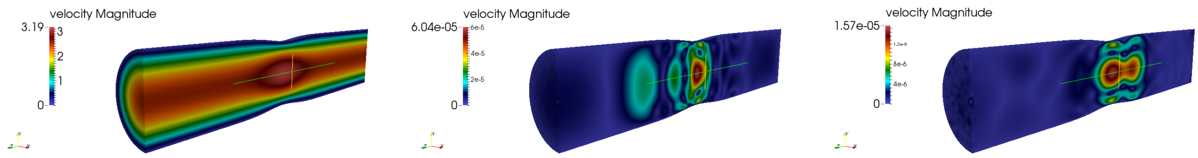

(a) FE velocity magnitude. (b) G-RB velocity error magnitude. (c) aLS-RB velocity error magnitude.

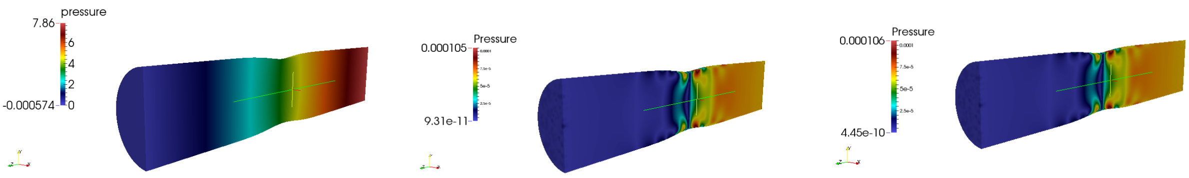

(d) FE pressure (e) G-RB norm of pressure error. (f) aLS-RB norm of pressure error.

Figure 5: FE solution and G-RB and aLS-RB errors for $\boldsymbol{\mu} = (2.7, 0.12)$.

and solving the FE problems to compute the deformation $\mathbf{d}_h^{\boldsymbol{\mu}}$ and the lifting function $\mathbf{r}_h^{\boldsymbol{\mu}}$, which on average requires 2.5 seconds in total. In our implementation this is included in the assembly of the RB matrix, whose required computational time is reported in Fig. 9. By substituting in the simulation pipeline the assembly and solution of the FE problems to compute $\mathbf{d}_h^{\boldsymbol{\mu}}$ and $\mathbf{r}_h^{\boldsymbol{\mu}}$ with a less expensive model, e.g. by using a cheap RB approximation for the computation of $\mathbf{d}_h^{\boldsymbol{\mu}}$ and $\mathbf{r}_h^{\boldsymbol{\mu}}$, one can compute an accurate solution with the aLS-RB method, which needs only 5% of the time required by the FE simulation.

In Table 3, for the three methods examined, we compare the minimum computational time to compute a RB approximation whose residual r_{RB} is lower than a fixed target accuracy. The two versions of the aLS-RB method confirm to reach a better accuracy in a lower time. The 'x' in the the G-RB column states that the accuracy 10^{-4} is not reached when this method with the given tolerance values δ_{RB}, $\delta_{\text{deim}} = 10^{-l}$, $l = 2, 3, 4, 5, 6$. Therefore, one should further decrease δ_{RB} and δ_{deim} to compute a more accurate solution.

Table 3: Computational time (seconds) required by the RB methods to compute a solution satisfying a target accuracy.

Accuracy	**G-RB**	**aLS-RB ($\mathbf{X}_h^0$)**	**aLS-RB ($\mathbf{P}_X^0$)**
1e-01	3.73	3.74	3.74
1e-02	3.93	3.74	3.74
1e-03	3.99	3.76	3.77
1e-04	x	4.14	3.91

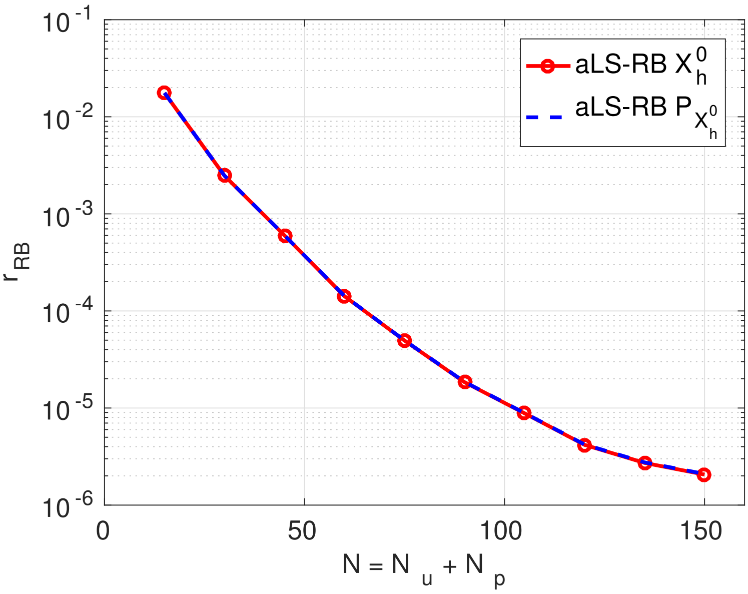

Figure 6: Convergence of the residual in norm $(\mathbf{X}_h^{\boldsymbol{\mu}})^{-1}$ vs the number of basis functions $N = N_u + N_p$ for the two case aLSRB (with $\mathbf{X}_h^0$ and $\mathbf{P}_{\mathbf{X}_h^0}$). Results computed with $\delta_{\text{deim}} = 10^{-8}$.

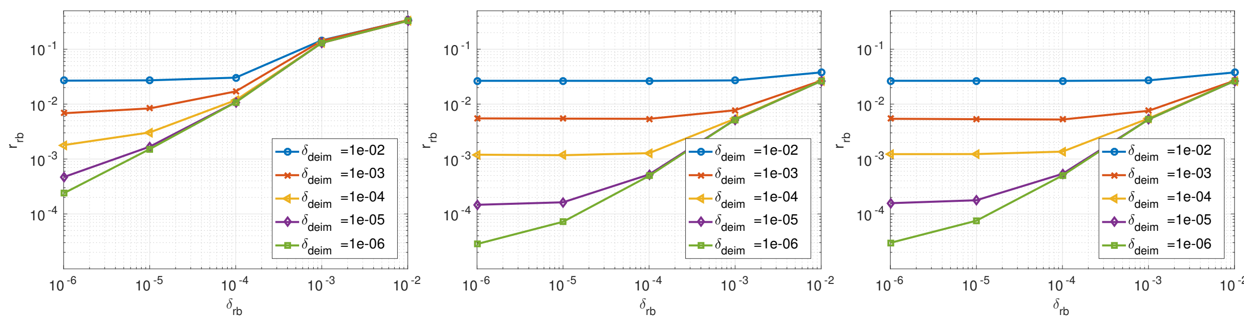

(a) GRB. (b) aLSRB ($\mathbf{X}_h^0$). (c) aLSRB ($\mathbf{P}_{\mathbf{X}_h^0}$).

Figure 7: Residuals in norm $(\mathbf{X}_h^{\boldsymbol{\mu}})^{-1}$ vs δ_{RB} for $\delta_{\text{deim}} = 10^{-l}$, $l = 2, 3, 4, 5, 6$.

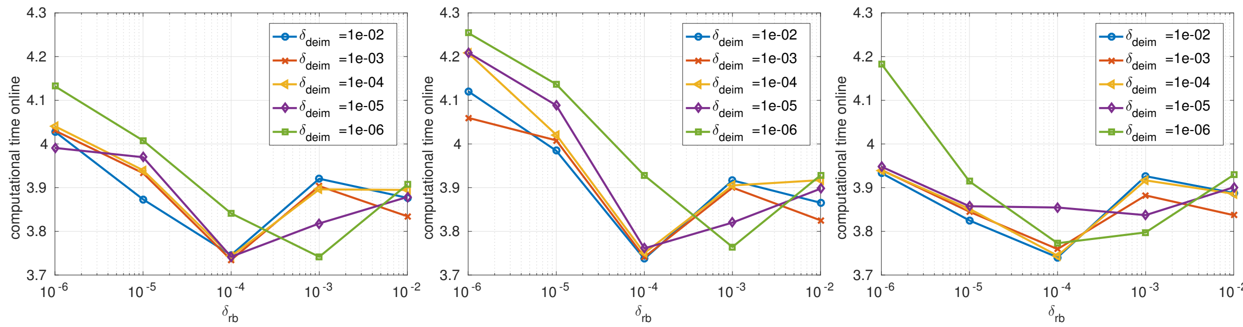

(a) GRB. (b) aLSRB ($\mathbf{X}_h^0$). (c) aLSRB ($\mathbf{P}_{\mathbf{X}_h^0}$).

Figure 8: Computational times (seconds) vs δ_{RB} for $\delta_{\text{deim}} = 10^{-l}$, $l = 2, 3, 4, 5, 6$.

5 Conclusions

In this paper we have proposed a new algebraic PG-RB method which can be generally used when the problem is parametrized with respect to the shape of the computational domain, especially when an analytical dependence of the geometry from the parameters is not known a priori. When such a case occurs, the state of the art PG-RB methods are currently not exploitable, since they require an unbearable amount of computation to build the RB problem online due to the $\boldsymbol{\mu}-$dependence of the matrix $\mathbf{X}_h^{\boldsymbol{\mu}}$.

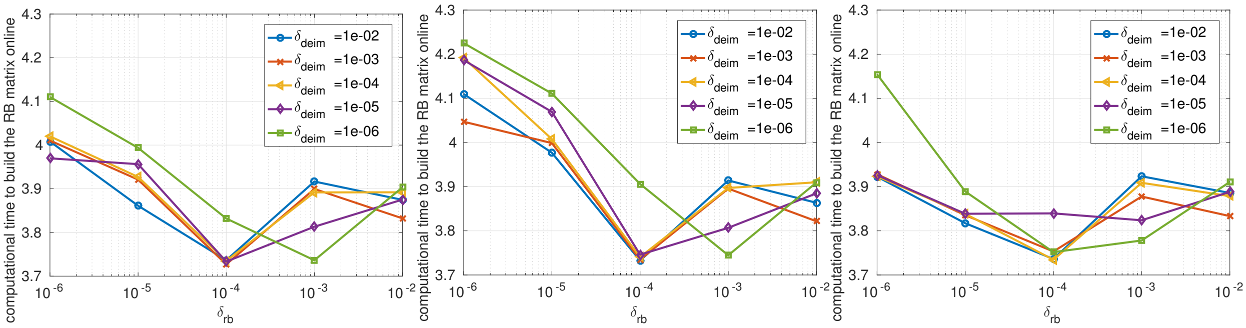

(a) GRB. (b) aLSRB ($\mathbf{X}_h^0$). (c) aLSRB ($\mathbf{P}_{\mathbf{X}_h^0}$).

Figure 9: Building time (seconds) for $\mathbf{A}_N^{\boldsymbol{\mu}}$ vs δ_{RB} for $\delta_{\text{deim}} = 10^{-l}$, $l = 2, 3, 4, 5, 6$.

The key idea of the proposed method relies on approximating the ($\boldsymbol{\mu}$-dependent) matrix $\mathbf{X}_h^{\boldsymbol{\mu}}$ used to build a standard LS-RB approximation, with a $\boldsymbol{\mu}-$independent matrix $\mathbf{P}_X$, giving birth to an algebraic LS-RB method which we called aLS-RB. We have analyzed its theoretical properties by providing well-posedness results and by comparing it with the state of the art techniques to deal with the same class of problems, i.e. a G-RB approximation with augmented velocity basis.

Furthermore, we have numerically investigated its properties, comparing the results with the ones obtained with the G-RB approximation. The aLS-RB method provides a system with lower dimension and requires a lower number of affine terms in the affine decomposition of the FE arrays to reach a prescribed accuracy. Finally, the results obtained with the aLS-RB method are more accurate and are computationally cheaper (both at the offline and online stages) than the ones obtained using the G-RB method with velocity enrichment. Theoretical findings and numerical results suggest that the proposed strategy provides a valuable paradigm for the efficient construction of a stable and accurate RB method for Stokes equations and, more generally speaking, weakly coercive and/or saddle-point problems.

Acknowledgements

The research of N. Dal Santo has been supported by the Swiss State Secretariat for Education, Research and Innovation (SERI), project No. C14.0068, in the framework of the COST action number TD1307. The second author thanks the Swiss National Science Foundation for support under the grant FNS 200021E-168311. We acknowledge the Swiss National Supercomputing Centre (CSCS) for providing the CPU resources under project ID s635.

References

[1] A. Abdulle and O. Budáč. A Petrov–Galerkin reduced basis approximation of the Stokes equation in parameterized geometries. *Comptes Rendus de Mathematiques*, 353(7):641–645, 2015.

[2] I. Babuška. Error-bounds for finite element method. *Numerische Mathematik*, 16(4):322–333, 1971.

[3] E. Bache, J. Vega, and A. Velazquez. Model reduction in the back step fluid–thermal problem with variable geometry. *International Journal of Thermal Sciences*, 49(12):2376–2384, 2010.

[4] F. Ballarin, A. Manzoni, A. Quarteroni, and G. Rozza. Supremizer stabilization of POD–Galerkin approximation of parametrized steady incompressible Navier–Stokes equations. *International Journal for Numerical Methods in Engineering*, 102(5):1136–1161, 2015.

[5] M. Barrault, Y. Maday, N. C. Nguyen, and A. T. Patera. An 'empirical interpolation' method: application to efficient reduced-basis discretization of partial differential equations. *C. R. Math. Acad. Sci. Paris*, 339(9):667–672, 2004.

[6] M. Benzi, G. H. Golub, and J. Liesen. Numerical solution of saddle point problems. *Acta numerica*, 14:1–137, 2005.

[7] M. Benzi and A. J. Wathen. Some preconditioning techniques for saddle point problems. In *Model order reduction: theory, research aspects and applications*, pages 195–211. Springer Berlin Heidelberg, 2008.

[8] M. Bergmann, C.-H. Bruneau, and A. Iollo. Enablers for robust POD models. *Journal of Computational Physics*, 228(2):516 – 538, 2009.

[9] L. Bertagna, S. Deparis, L. Formaggia, D. Forti, and A. Veneziani. The Lifev library: engineering mathematics beyond the proof of concept. *submitted*, 2017.

[10] F. Brezzi. On the existence, uniqueness and approximation of saddle-point problems arising from lagrangian multipliers. *Revue française d'automatique, informatique, recherche opérationnelle. Analyse numérique*, 8(R2):129–151, 1974.

[11] F. Brezzi and K.-J. Bathe. A discourse on the stability conditions for mixed finite element formulations. *Computer methods in applied mechanics and engineering*, 82(1-3):27–57, 1990.

[12] A. Caiazzo, T. Iliescu, V. John, and S. Schyschlowa. A numerical investigation of velocity–pressure reduced order models for incompressible flows. *Journal of Computational Physics*, 259(Supplement C):598 – 616, 2014.

[13] C. Canuto, M. Y. Hussaini, A. Quarteroni, and A. Thomas Jr. *Spectral methods in fluid dynamics*. Springer Science & Business Media, 2012.

[14] K. Carlberg, C. Bou-Mosleh, and C. Farhat. Efficient non-linear model reduction via a least-squares Petrov–Galerkin projection and compressive tensor approximations. *International Journal for Numerical Methods in Engineering*, 86(2):155–181, 2011.

[15] S. Chaturantabut and D. C. Sorensen. Nonlinear model reduction via discrete empirical interpolation. *SIAM Journal on Scientific Computing*, 32(5):2737–2764, 2010.

[16] W. Dahmen, C. Huang, C. Schwab, and G. Welper. Adaptive petrov–galerkin methods for first order transport equations. *SIAM journal on numerical analysis*, 50(5):2420–2445, 2012.

[17] S. Deparis. Reduced basis error bound computation of parameter-dependent Navier–Stokes equations by the natural norm approach. *SIAM Journal of Numerical Analysis*, 46(4):2039–2067, 2008.

[18] S. Deparis and G. Rozza. Reduced basis method for multi-parameter-dependent steady Navier-Stokes equations: Applications to natural convection in a cavity. *Journal of Computational Physics*, 228(12):4359–4378, 2009.

[19] P. Díez, S. Zlotnik, and A. Huerta. Generalized parametric solutions in stokes flow. *Computer Methods in Applied Mechanics and Engineering*, 326(Supplement C):223 – 240, 2017.

[20] H. C. Elman and V. Forstall. Numerical solution of the parameterized steady-state navier–stokes equations using empirical interpolation methods. *Computer Methods in Applied Mechanics and Engineering*, 317:380 – 399, 2017.

[21] H. C. Elman, D. J. Silvester, and A. J. Wathen. Finite elements and fast iterative solvers: with applications in incompressible fluid dynamics, 2005.

[22] M. W. Gee, C. M. Siefert, J. J. Hu, R. S. Tuminaro, and M. G. Sala. Ml 5.0 smoothed aggregation user's guide. Technical report, SAND2006-2649, Sandia National Laboratories, 2006.

[23] A.-L. Gerner and K. Veroy. Certified reduced basis methods for parametrized saddle point problems. *SIAM J. Sci. Comput.*, 34(5):A2812–A2836, 2012.

[24] J. S. Hesthaven, G. Rozza, and B. Stamm. Certified reduced basis methods for parametrized partial differential equations. *SpringerBriefs in Mathematics*, 2016.

[25] K. Kunisch and S. Volkwein. Galerkin proper orthogonal decomposition methods for a general equation in fluid dynamics. *SIAM J. Numerical Analysis*, 40(2):492–515, 2002.

[26] A. Manzoni. An efficient computational framework for reduced basis approximation and a posteriori error estimation of parametrized Navier-Stokes flows. *ESAIM: Mathematical Modelling and Numerical Analysis*, 48(4):1199–1226, 2014.

[27] A. Manzoni and F. Negri. Efficient reduction of pdes defined on domains with variable shape. In *Model Reduction of Parametrized Systems*, pages 183–199. Springer, Cham, 2017.

[28] A. Manzoni, A. Quarteroni, and G. Rozza. Shape optimization of cardiovascular geometries by reduced basis methods and free-form deformation techniques. *Int. J. Numer. Methods Fluids*, 70(5):646–670, 2012.

[29] F. Negri. *Efficient Reduction Techniques for the Simulation and Optimization of Parametrized Systems*. PhD thesis, EPFL, 2015.

[30] F. Negri, A. Manzoni, and D. Amsallem. Efficient model reduction of parametrized systems by matrix discrete empirical interpolation. *Journal of Computational Physics*, 303:431–454, 2015.

[31] F. Negri, A. Manzoni, and G. Rozza. Reduced basis approximation of parametrized optimal flow control problems for the Stokes equations. *Computers & Mathematics with Applications*, 69:319–336, 2015.

[32] A. Quarteroni. *Numerical Models for Differential Problems*, volume 9 of *Modeling, Simulation and Applications (MS&A)*. Springer-Verlag Italia, Milano, 2nd edition, 2014.

[33] A. Quarteroni, A. Manzoni, and F. Negri. *Reduced Basis Methods for Partial Differential Equations: An Introduction*, volume 92. Springer, 2016.

[34] A. Quarteroni and G. Rozza. Numerical solution of parametrized Navier–Stokes equations by reduced basis methods. *Numerical Methods for Partial Differential Equations*, 23(4):923–948, 2007.

[35] A. Quarteroni and A. Valli. *Numerical approximation of partial differential equations*. Springer Science & Business Media, 2008.

[36] M. Rehman, T. Geenen, C. Vuik, G. Segal, and S. MacLachlan. On iterative methods for the incompressible Stokes problem. *International Journal for Numerical methods in fluids*, 65(10):1180–1200, 2011.

[37] G. Rozza. Reduced basis methods for Stokes equations in domains with non-affine parameter dependence. *Computing and Visualization in Science*, 12(1):23–35, Jan 2009.

[38] G. Rozza, D. Huynh, and A. Manzoni. Reduced basis approximation and error bounds for Stokes flows in parametrized geometries: roles of the inf–sup stability constants. *Numerische Mathematik*, 125(1):115–152, 2013.

[39] G. Rozza and K. Veroy. On the stability of the reduced basis method for Stokes equations in parametrized domains. *Computer methods in applied mechanics and engineering*, 196(7):1244–1260, 2007.

[40] A. Toselli and O. B. Widlund. *Domain decomposition methods: algorithms and theory*. Springer series in computational mathematics. Springer, Berlin, 2005.

[41] J. Weller, E. Lombardi, M. Bergmann, and A. Iollo. Numerical methods for low-order modeling of fluid flows based on POD. *Int. J. Numer. Methods Fluids*, 63(2):249–268, 2010.

A Proofs of the results in Section 3.3.2

In the proofs we will omit the apex $\boldsymbol{\mu}$ for the sake of clearness, i.e. $\mathbf{X}_h = \mathbf{X}_h^{\boldsymbol{\mu}}$.

A.1 Lemma 3.2

Proof. Being $\mathbf{X}_h$ and $\mathbf{P}_X$ symmetric and positive definite, for any $\mathbf{y} \in \mathbb{R}^{N_h}$ it holds

$$\begin{aligned}\|\mathbf{y}\|^2_{\mathbf{X}_h} &= \left(\mathbf{X}_h^{1/2}\mathbf{y}, \mathbf{X}_h^{1/2}\mathbf{y}\right)_2 = \left(\mathbf{P}_X^{-1/2}\mathbf{P}_X\mathbf{P}_X^{-1/2}\mathbf{X}_h^{1/2}\mathbf{y}, \mathbf{X}_h^{1/2}\mathbf{y}\right)_2 = \left(\mathbf{P}_X\mathbf{P}_X^{-1/2}\mathbf{X}_h^{1/2}\mathbf{y}, \mathbf{P}_X^{-1/2}\mathbf{X}_h^{1/2}\mathbf{y}\right)_2 \\ &= \left(\mathbf{P}_X^{-1/2}\mathbf{X}_h^{1/2}\mathbf{y}, \mathbf{P}_X^{-1/2}\mathbf{X}_h^{1/2}\mathbf{y}\right)_{\mathbf{P}_X} = \|\mathbf{P}_X^{-1/2}\mathbf{X}_h^{1/2}\mathbf{y}\|^2_{\mathbf{P}_X} \le \|\mathbf{P}_X^{-1/2}\mathbf{X}_h^{1/2}\|^2_{\mathbf{P}_X}\|\mathbf{y}\|^2_{\mathbf{P}_X},\end{aligned}$$

and there exists an element $\mathbf{y}_0 \in \mathbb{R}^{N_h}$ where equality is reached. This leads to an optimal $C = \|\mathbf{P}_X^{-1/2}\mathbf{X}_h^{1/2}\|_{\mathbf{P}_X}$. Similarly, by inverting the roles of $\mathbf{P}_X$ and $\mathbf{X}_h$ and following the same argument, we have that $c = 1/\|\mathbf{X}_h^{-1/2}\mathbf{P}_X^{1/2}\|_{\mathbf{X}_h}$. □

A.2 Lemma 3.3

Proof. We rewrite the optimal values for C and c as it follows

$$
\begin{aligned}
C^2 &= \|\mathbf{P}_X^{-1/2}\mathbf{X}_h^{1/2}\|_{\mathbf{P}_X}^2 = \sup_{\mathbf{y}\in\mathbb{R}^{N_h},\mathbf{y}\neq\mathbf{0}} \frac{\|\mathbf{P}_X^{-1/2}\mathbf{X}_h^{1/2}\mathbf{y}\|_{\mathbf{P}_X}^2}{\|\mathbf{y}\|_{\mathbf{P}_X}^2} \\
&= \sup_{\mathbf{y}\in\mathbb{R}^{N_h},\mathbf{y}\neq\mathbf{0}} \frac{(\mathbf{P}_X^{-1/2}\mathbf{X}_h^{1/2}\mathbf{y},\mathbf{P}_X^{-1/2}\mathbf{X}_h^{1/2}\mathbf{y})_{\mathbf{P}_X}}{(\mathbf{y},\mathbf{y})_{\mathbf{P}_X}} = \sup_{\mathbf{y}\in\mathbb{R}^{N_h},\mathbf{y}\neq\mathbf{0}} \frac{(\mathbf{X}_h^{1/2}\mathbf{y},\mathbf{X}_h^{1/2}\mathbf{y})_2}{(\mathbf{P}_X^{1/2}\mathbf{y},\mathbf{P}_X^{1/2}\mathbf{y})_2} \\
&= \sup_{\mathbf{y}\in\mathbb{R}^{N_h},\mathbf{y}\neq\mathbf{0}} \frac{(\mathbf{X}_h^{1/2}\mathbf{P}_X^{-1/2}\mathbf{P}_X^{1/2}\mathbf{y},\mathbf{X}_h^{1/2}\mathbf{P}_X^{-1/2}\mathbf{P}_X^{1/2}\mathbf{y})_2}{(\mathbf{P}_X^{1/2}\mathbf{y},\mathbf{P}_X^{1/2}\mathbf{y})_2} \\
&= \sup_{\mathbf{w}\in\mathbb{R}^{N_h},\mathbf{w}\neq\mathbf{0}} \frac{(\mathbf{X}_h^{1/2}\mathbf{P}_X^{-1/2}\mathbf{w},\mathbf{X}_h^{1/2}\mathbf{P}_X^{-1/2}\mathbf{w})_2}{(\mathbf{w},\mathbf{w})_2} = \sup_{\mathbf{w}\in\mathbb{R}^{N_h},\mathbf{w}\neq\mathbf{0}} \frac{\|\mathbf{X}_h^{1/2}\mathbf{P}_X^{-1/2}\mathbf{w}\|_2^2}{\|\mathbf{w}\|_2^2} \\
&= \|\mathbf{X}_h^{1/2}\mathbf{P}_X^{-1/2}\|_2^2. \qquad (45)
\end{aligned}
$$

Similarly, we have that $\|\mathbf{X}_h^{-1/2}\mathbf{P}_X^{1/2}\|_{\mathbf{X}_h} = \|\mathbf{P}_X^{1/2}\mathbf{X}_h^{-1/2}\|_2$, yielding

$$
\begin{aligned}
\frac{c}{C} &= \left(\|\mathbf{X}_h^{-1/2}\mathbf{P}_X^{1/2}\|_{\mathbf{X}_h}\|\mathbf{P}_X^{-1/2}\mathbf{X}_h^{1/2}\|_{\mathbf{P}_X}\right)^{-1} = \left(\|\mathbf{P}_X^{1/2}\mathbf{X}_h^{-1/2}\|_2\|\mathbf{X}_h^{1/2}\mathbf{P}_X^{-1/2}\|_2\right)^{-1} \\
&= \left[\mathcal{K}_2(\mathbf{X}_h^{1/2}\mathbf{P}_X^{-1/2})\right]^{-1} = \left[\mathcal{K}_2(\mathbf{P}_X^{1/2}\mathbf{X}_h^{-1/2})\right]^{-1},
\end{aligned}
$$

where the last two relations are both used to find different equalities. Next, by recalling the definition of condition number (with respect to the Euclidean norm) $\mathcal{K}_2$ for a matrix, we obtain

$$
\begin{aligned}
\mathcal{K}_2(\mathbf{X}_h^{1/2}\mathbf{P}_X^{-1/2}) &= \sqrt{\frac{\lambda_{\max}\left((\mathbf{X}_h^{1/2}\mathbf{P}_X^{-1/2})^T\mathbf{X}_h^{1/2}\mathbf{P}_X^{-1/2}\right)}{\lambda_{\min}\left((\mathbf{X}_h^{1/2}\mathbf{P}_X^{-1/2})^T\mathbf{X}_h^{1/2}\mathbf{P}_X^{-1/2}\right)}} = \sqrt{\frac{\lambda_{\max}\left(\mathbf{P}_X^{-1/2}\mathbf{X}_h\mathbf{P}_X^{-1/2}\right)}{\lambda_{\min}\left(\mathbf{P}_X^{-1/2}\mathbf{X}_h\mathbf{P}_X^{-1/2}\right)}} \\
&= \sqrt{\mathcal{K}_2\left(\mathbf{P}_X^{-1/2}\mathbf{X}_h\mathbf{P}_X^{-1/2}\right)},
\end{aligned}
$$

which verifies the second equality of (42). On the other hand we have

$$
\begin{aligned}
\mathcal{K}_2(\mathbf{P}_X^{1/2}\mathbf{X}_h^{-1/2}) &= \sqrt{\mathcal{K}_2\left(\mathbf{X}_h^{-1/2}\mathbf{P}_X\mathbf{X}_h^{-1/2}\right)} = \sqrt{\|\mathbf{X}_h^{-1/2}\mathbf{P}_X\mathbf{X}_h^{-1/2}\|_2\|\mathbf{X}_h^{1/2}\mathbf{P}_X^{-1}\mathbf{X}_h^{1/2}\|_2} \\
&= \sqrt{\|\mathbf{X}_h^{-1}\mathbf{P}_X\|_{\mathbf{X}_h}\|\mathbf{P}_X^{-1}\mathbf{X}_h\|_{\mathbf{X}_h}} = \sqrt{\mathcal{K}_{\mathbf{X}_h}(\mathbf{P}_X^{-1}\mathbf{X}_h)},
\end{aligned}
$$

where we have used that $\|\mathbf{X}_h^{-1/2}\mathbf{P}_X\mathbf{X}_h^{-1/2}\|_2 = \|\mathbf{X}_h^{-1}\mathbf{P}_X\|_{\mathbf{X}_h}$ and $\|\mathbf{X}_h^{1/2}\mathbf{P}_X^{-1}\mathbf{X}_h^{1/2}\|_2 = \|\mathbf{P}_X^{-1}\mathbf{X}_h\|_{\mathbf{X}_h}$; these latter relationships are verified similarly to (45), and their proof can therefore be omitted. □

Recent publications:

INSTITUTE of MATHEMATICS
MATHICSE Group

Ecole Polytechnique Fédérale (EPFL)

CH-1015 Lausanne

2017

09.2017 PABLO ANTOLIN, ANNALISA BUFFA, MATHIEU FABRE:
A priori error for unilateral contact problems with Lagrange multipliers and IsoGeometric Analysis

10.2017 MICHELE PISARONI, FABIO NOBILE, PENELOPE LEYLAND:
Continuation Multi-A priori error for unilateral contact problems with Lagrange multipliers and IsoGeometric Analysis

11.2017 ANDREAS FROMMER, CLAUDIA SCHIMMEL, MARCEL SCHWEITZER:
Bounds for the decay of the entries in inverses and Cauchy-Stieltjes functions of sparse, normal matrices

12.2017 SEBASTIAN KRUMSCHEID, FABIO NOBILE:
Multilevel Monte Carlo approximation of functions,

13.2017 R.N. SIMPSON, Z. LIU, R. VÁZQUEZ, J.A. EVANS:
An isogeometric boundary element method for electromagnetic scattering with compatible B-spline discretization

14.2017 NICCOLO DAL SANTO, SIMONE DEPARIS, ANDREA MANZONI:
A numerical investigation of multi space reduced basis preconditioners for parametrized elliptic advection-diffusion

15.2017 ASSYR ABDULLE, TIMOTHÉE POUCHON:
Effective models for long time wave propagation in locally periodic media

16.2017 ASSYR ABDULLE, MARCUS J. GROTE, ORANE JECKER:
FE-HMM for elastic waves in heterogeneous media

17.2017 JOHN A. EVANS, MICHAEL A. SCOTT, KENDRICK SHEPHERD, DEREK THOMAS, RAFAEL VÁZQUEZ:
Hierarchical B-spline complexes of discrete differential forms

18.2017 ELEONORA MUSHARBASH, FABIO NOBILE:
Symplectic dynamical low rank approximation of wave equations with random parameters

19.2017 ASSYR ABDULLE, IBRAHIM ALMUSLIMANI, GILLES VILMART:
Optimal explicit stabilized integrator of weak order one for stiff and ergodic stochastic differential equations

20.2017 ABDUL-LATEEF HAJI-ALI, FABIO NOBILE, RAÚL TEMPONE, SÖREN WOLFERS:
Multilevel weighted least squares polynomial approximation

21.2017 NICCOLO DAL SANTO, SIMONE DEPARIS, ANDREA MANZONI, ALFIO QUARTERONI:
An algebraic least squares reduced basis method for the solution of parametrized Stokes equations

***